A TEMPERATURE AND PRESSURE DEPENDENT KINETICS STUDY OF THE GAS-PHASE REACTIONS OF BROMINE ($^2P_{3/2}$) AND CHLORINE (^2P_J) ATOMS WITH METHYLVINYL KETONE

A Thesis
Presented to
The Academic Faculty

By

Dow T. Huskey

In Partial Fulfillment
Of the Requirements for the Degree
Master of Science Chemistry

Georgia Institute of Technology
August 2008

A TEMPERATURE AND PRESSURE DEPENDENT KINETICS STUDY OF THE GAS-PHASE REACTIONS OF BROMINE ($^2P_{3/2}$) AND CHLORINE (^2P_J) ATOMS WITH METHYLVINYL KETONE

Approved by:

Dr. Paul H. Wine, Advisor
School of Chemistry and Biochemistry
School of Earth and Atmospheric Sciences
Georgia Institute of Technology

Dr. Jean-Luc Brédas
School of Chemistry and Biochemistry
Georgia Institute of Technology

Dr. Rigoberto Hernandez
School of Chemistry and Biochemistry
Georgia Institute of Technology

Date Approved: June 30, 2008

ACKNOWLEDGEMENTS

First and foremost I would like to express my sincere gratitude to my advisor, Dr. Paul Wine, for giving me an opportunity to join his research group as well as for providing encouragement, support, and thoughtful suggestions during my time in the group.

Secondly, I offer my profound thanks to the group's Sr. Research Scientist, Dr. Mike Nicovich, for his guidance, advice, and supervision while conducting this and other research. Without his help, this thesis would not have been possible.

I want to recognize the efforts of Dr. Mike McKee of Auburn University who provided all the theoretical information including important calculations, figures, and other data.

I also want to gratefully acknowledge my chemistry department committee professors, Dr. Jean-Luc Brédas and Dr. Rigoberto Hernandez, who not only took their time to review this thesis but also provided me with exceptional instruction in lecture courses.

During my time in the group, I was blessed to have worked with several talented colleagues and good friends: Katie Olsen, Zhijun Zhao, Venus Dookwah-Roberts, and Patrick Laine. I'm grateful to have had the opportunity to participate in the Wine Group and I wish the group continued success in the future.

Funding for this project was graciously accepted by generous grants from NASA and NSF.

Additional thanks to Josh Allen, an undergraduate student at Georgia Tech, for his contributions in the lab.

To my friend Frannie, as always thank you for your friendship and encouragement before and during my time at Georgia Tech.

I also want to thank my brother, Whit, for his confidence in me to do this and for being my life-long best friend.

Most importantly, I want to thank my parents for their unending generosity, love, and support. I could never have completed this without you. This work is for you.

TABLE OF CONTENTS

ACKNOWLEDGEMENTS……(iii)

LIST OF TABLES……(vii)

LIST OF FIGURES……(viii)

LIST OF SYMBOLS……(ix)

SUMMARY……..(xii)

CHAPTER 1: INTRODUCTION……..(1)

CHAPTER 2: EXPERIMENTAL TECHNIQUE……..(7)

CHAPTER 3: RESULTS AND DISCUSSION OF Br + $CH_3C(O)CH=CH_2$ EXPERIMENTS……..(14)

3.1 Kinetics at 200 K < T < 250K……(15)
3.2 $CH_3C(O)CHCH_2$-Br Thermochemistry: Second-Law Analysis……..(21)
3.3 $CH_3C(O)CHCH_2$-Br Thermochemistry: Third-Law Analysis……(21)
3.4 Literature Comparison……(25)

CHAPTER 4: RESULTS AND DISCUSSION OF Cl + $CH_3C(O)CH=CH_2$ EXPERIMENTS……..(32)

4.1 Kinetics at 600 K < T < 760 K ……..(33)
4.2 Kinetics at 405 K < T < 510 K……...(37)
4.3 Kinetics at 210 K < T < 365 K……...(41)
4.4 $CH_3C(O)CHCH_2$-Cl Corrections to Rate Cofficients……...(42)
4.5 $CH_3C(O)CHCH_2$-Cl Thermochemistry: Second-Law Analysis……..(48)
4.6 $CH_3C(O)CHCH_2$-Cl Thermochemistry: Third-Law Analysis……(50)
4.7 Literature Comparison……(54)

CHAPTER 5: CONCLUSIONS……(61)

REFERENCES……(67)

LIST OF TABLES

Table 1 Results for the Br + $CH_3C(O)CH=CH_2 \leftrightarrow CH_3C(O)CHCH_2$-Br reaction at 200 K < T < 250 K……(19)

Table 2 Summary of parameters used in calculations of absolute entropies and heat capacity corrections for the Br + $CH_3C(O)CH=CH_2 \leftrightarrow CH_3C(O)CHCH_2$-Br reaction……(26)

Table 3 Thermochemical parameters for the reaction Br + $CH_3C(O)CH=CH_2 \leftrightarrow CH_3C(O)CHCH_2$-Br……..(27)

Table 4 Results for the Cl + $CH_3C(O)CH=CH_2 \rightarrow \dot{C}H_2C(O)CH=CH_2$ + HCl reaction at 600 K < T < 760 K……..(38)

Table 5 Results for the Cl + $CH_3C(O)CH=CH_2 \leftrightarrow CH_3C(O)CHCH_2$-Cl reaction at 405 K < T < 510 K……(43)

Table 6 Results for the Cl + $CH_3C(O)CH=CH_2 \rightarrow CH_3C(O)CHCH_2$-Cl reaction at 210 K < T < 365 K……...(46)

Table 7 Summary of parameters used in calculations of absolute entropies and heat capacity corrections for the Cl + $CH_3C(O)CH=CH_2 \leftrightarrow CH_3C(O)CHCH_2$-Cl reaction……..(53)

Table 8 Thermochemical parameters for the reaction Cl + $CH_3C(O)CH=CH_2 \leftrightarrow CH_3C(O)CHCH_2$-Cl……..(54)

Table 9 Comparison of results for the Cl + $CH_3C(O)CH=CH_2 \leftrightarrow CH_3C(O)CHCH_2$-Cl reaction from this study to existing literature studies……..(59)

LIST OF FIGURES

Figure 1 Schematic diagram of our Laser Flash Photolysis – Resonance Fluorescence (LFP-RF) apparatus……..(8)

Figure 2 Typical Br atom temporal profiles observed in this study……..…(18)

Figure 3 Van't Hoff Plot for the Br + $CH_3C(O)CH=CH_2$ ↔ $CH_3C(O)CHCH_2$-Br equilibrium……..……(22)

Figure 4 Structure for $CH_3C(O)CHCH_2$-Br provided by Mike McKee of Auburn University from *ab initio* calculations showing Br addition to the terminal carbon on the double bond……..(24)

Figure 5 Typical Cl temporal profiles observed at 600 K < T < 760 K……..(35)

Figure 6 Plots of k' vs [MVK] for data obtained at 600 K < T < 760 K……...(36)

Figure 7 Corrected Arrhenius Plot for the Cl + $CH_3C(O)CH=CH_2$ → $\dot{C}H_2C(O)CH=CH_2$ + HCl reaction……...(39)

Figure 8 Van't Hoff Plot for the Cl + $CH_3C(O)CH=CH_2$ ↔ $CH_3C(O)CHCH_2$-Cl equilibrium……..……...(49)

Figure 9 Structure for the Cl + MVK adduct provided by Mike McKee of Auburn University from *ab initio* calculations showing Cl addition to the terminal and internal carbon on the double bond……..(51)

LIST OF SYMBOLS

Symbol	Definition	Units
(^2P_J)	Term symbol	
A	Arrhenius pre-exponential factor	cm^3 $molecule^{-1}$ s^{-1}
atm	Atmosphere	
Br	Bromine	
cal	Calorie	
Cl	Chlorine	
cm^3	Centimeters cubed	
$\Delta_f H$	Enthalpy of formation	kcal mol^{-1}
$\Delta_r H$	Enthalpy of reaction	kcal mol^{-1}
$\Delta_r S$	Entropy of reaction	cal mol^{-1} K^{-1}
ε	Equilibrium adduct concentration ratio	
Ea	Activation energy	
FT-IR	Fourier Transform Infrared	
h	Plank's constant, 6.626×10^{-34}	J s
Hz	Hertz	s^{-1}
J	Joule	
K	Kelvin	

K_C	Equilibrium constant	cm^3 $molecule^{-1}$
kcal	Kilocalorie	
k_i	Bimolecular rate coefficient Unimolecular rate coefficient	cm^3 $molecule^{-1}$ s^{-1} s^{-1}
K_P	Equilibrium constant	atm^{-1}
λ_1	Fit parameter for the double exponential equation I	s^{-1}
λ_2	Fit parameter for the double exponential equation I	s^{-1}
LFP	Laser Flash Photolysis	
mbar	Millibar	
mJ	Millijoule	
mol	Mole	
MVK	Methylvinyl ketone	
nm	Nanometer	
ns	Nanosecond	
P	Pressure	atm
Q	Fit parameter for the double exponential equation I	s^{-1}
R	Universal gas constant, 8.314	J mol^{-1} K^{-1}
RF	Resonance Fluorescence	
s	Seconds	
σ	Standard deviation	

S_0	Signal level at time = 0	counts
S_t	Signal level at time = t	counts
t	Time	s
T	Temperature	
UHP	Ultra high purity	
ν	Frequency	s^{-1}

SUMMARY

A laser flash photolysis – resonance fluorescence (LFP-RF) technique has been employed to study the kinetics of the reactions of methylvinyl ketone ($CH_3C(O)CH=CH_2$, MVK) with atomic bromine (Br) and atomic chlorine (Cl) as a function of temperature (203 – 755 K) and pressure (12 – 600 Torr) in nitrogen (N_2) bath gas. Over the temperature range 200 K < T < 250 K for the reaction of Br with MVK, measured rate coefficients were pressure dependent suggesting the formation of an adduct. The adduct undergoes dissociation on the time scale of the experiments (< 0.1 s) and establishes an equilibrium between Br, MVK, and MVK–Br. At temperatures above 298 K no reaction of Br with MVK was observed. Similarly, over the temperature range 405 K < T < 510 K, the reaction of Cl with MVK shows similar kinetics to that of Br and MVK suggesting an equilibrium is established. Equilibrium constants for adduct dissociation and formation are determined from the forward and reverse rate coefficients in both reactions. Second and third-law analyses of the equilibrium reactions for Br with MVK and Cl with MVK were carried out. In the case of the reaction of Br with MVK the analyses yielded the following thermochemical values, $\Delta_rH°_{298} = -11.4 \pm 0.8$ kcal mol^{-1}, $\Delta_rH°_0 = -$

11.0 ± 0.7 kcal mol^{-1}, $\Delta_rS°_{298}$ = –25.0 ± 2.6 cal mol^{-1} K^{-1}; for the reaction of Cl with MVK, $\Delta_rH°_{298}$ = –25.0 ± 2.0 kcal mol^{-1}, $\Delta_rH°_0$ = –24.5 ± 1.9 kcal mol^{-1}, $\Delta_rS°_{298}$ = –26.6 ± 3.1 cal mol^{-1} K^{-1}. *Ab initio* calculations for these reactions are also presented in this study. Excellent agreement is observed between theory and experiment. Additionally, a reaction of Cl with MVK was observed over the temperature ranges 600 K < T < 760 K and 210 K < T < 365 K. At the lower temperatures, measured rate coefficients are also pressure dependent, however, the adduct remained stable. At the highest temperatures, the measured rate coefficients were pressure independent, suggesting hydrogen abstraction as the dominant reaction pathway. The following Arrhenius expression describes all kinetic data over the 600 K < T < 760 K temperature range: $k_3(T)$ = (5.10 ± 1.15) x 10^{-11}exp[–(1615 ± 96)/T] cm^3 $molecule^{-1}$ s^{-1}. Energetics obtained from *ab initio* calculations suggest that only abstraction of the methyl hydrogen is likely to occur at a measurable rate in the temperature range investigated.

CHAPTER 1

INTRODUCTION

This thesis provides specific kinetic rate data and represents the first study to explore both temperature and pressure variations in rate coefficients for the reactions of methylvinyl ketone ($CH_3C(O)CH=CH_2$, MVK) with atomic bromine (Br) and atomic chlorine (Cl). It provides rate coefficients that will be useful in accounting for additional sinks for MVK in the atmosphere. These rate coefficients can be used for modeling atmospheric processes which may help make predictions for future climate change and to better understand ozone depletion. Additionally, this work also helps to quantify our understanding of halogen reactions with unsaturated species in general by comparing rate coefficients and bond strengths from this work to existing studies as well as to quantum chemical calculations. The specific reactions studied are shown below:

$$Br + CH_3C(O)CH=CH_2 + N_2 \leftrightarrow CH_3C(O)CHCH_2\text{-}Br + N_2 \quad (1, -1)$$

$$Cl + CH_3C(O)CH=CH_2 + N_2 \leftrightarrow CH_3C(O)CHCH_2\text{-}Cl + N_2 \quad (2, -2)$$

$$Cl + CH_3C(O)CH=CH_2 \rightarrow \dot{C}H_2C(O)CH=CH_2 + HCl \quad (3)$$

Methylvinyl ketone is a first generation oxidation product of isoprene, the most abundant non-methane hydrocarbon in the troposphere *[Gierczak et al, 1997; Hsin et al, 2007; Isidorov et al., 1985]*. Isoprene's primary source is emission from trees and a number of other plant species. Isoprene plays a significant role in the formation of ozone in the troposphere *[Hsin et al, 2007]*. However, the importance of isoprene in the atmosphere cannot be fully encompassed without an understanding of the reactions of MVK.

Three reaction types are known to occur in the radical-initiated oxidation of MVK: electrophilic addition to the terminal or non-terminal carbon on the double bond and abstraction of one of the methyl hydrogens *[Ochando-Pardo et at., 2005];* the abstraction reaction is likely to be important only at high temperatures and/or very low pressures. The products of the oxidation of MVK can lead to the formation of glycolaldehyde, methylglyoxal, formaldehyde, peroxyacetyl nitrate (PAN), propene, and ozone *[Gierczak et al, 1997; Raber et al., 1995; Tuazon et al., 1989]*. Although tropospheric oxidation of MVK is primarily initiated by OH radicals *[Atkinson, 1986]* or photolysis *[Finlayson-Pitts et al., 2000],* reaction with halogen atoms may also play a role. In recent years there has been increased interest in reactive halogens, particularly Br and Cl.

Usually occurring in snow-pack, sea ice, or marine aerosols, molecular bromine (Br_2) is generated by heterogeneous processes from sea-salt bromide *[Tang et al., 1996; Vogt et al., 1996]*. Photolysis of gaseous Br_2 in these areas yields atomic Br which is a well known destroyer of ozone. Additionally, it has been postulated that micro algae in the Arctic emit bromoform ($CHBr_3$) which can be photolyzed into Br radicals during the polar sunrise *[Sturges et al., 1992; Sturges et al., 1993a,b]*. Model calculations have shown that high concentrations of Br are possible in the lower arctic atmosphere *[Barrie et al., 1988, Platt et al., 1995,* Ramacher et al., 1997*]*. The rate of reaction of Br with MVK, ~5.5 x 10^{-11} cm^3 $molecule^{-1}$ s^{-1} at 301 K and ~1 atm, estimated from this study, is similar to that of reaction with OH, 2.03 x 10^{-11} cm^3 $molecule^{-1}$ s^{-1} at 298 K and 100 Torr *[Gierczak et al, 1997]*. The reaction of Br with MVK could dominate the OH reaction in colder regions where Br atom concentrations can reach levels that are much higher than OH concentrations.

Atomic chlorine is believed to play and important role in oxidation of organics in marine and coastal environments, particularly in the early morning hours *[Ragains et al., 1997]*, where the Cl concentration may be as high as 10^4 – 10^5 atoms cm^{-3} *[Boundries et al., 2000; Pszenny et al., 1993; Wingenter et al., 2005],* i.e., only 1-2 orders of magnitude smaller than

typical OH concentrations *[Jobson et al., 1994; Singh et al., 1996a; Zhao et al., 2007]*. However, Cl atoms are not believed to compete with OH on a global scale *[Rudolph et al., 1996; Singh et al., 1996b]*. Nevertheless, the rate coefficient for the reaction of Cl with MVK, 1.49 x 10^{-10} cm^3 $molecule^{-1}$ s^{-1} at 297 K and 75 Torr determined by this study, is an order of magnitude faster than the rate coefficient of OH reaction with MVK, 2.03 x 10^{-11} cm^3 $molecule^{-1}$ s^{-1} at 298 K and 100 Torr *[Gierczak et al, 1997]*. Therefore, the removal of MVK by Cl is roughly the same where Cl concentrations are ~10^4 – 10^5 atoms cm^{-3}. While there is still some debate regarding the source of Cl in the atmosphere, a probable origin may be photodissociation of Cl_2 and $ClNO_2$ formed by heterogeneous reactions on the surfaces of moist sea salt particles *[Finlayson-Pitts et al., 1993]*.

This thesis represents the first direct study of the Br + MVK reaction. This reaction was studied over the temperature and pressure ranges 200 K < T < 250 K and 25 ≤ P ≤ 100 Torr in nitrogen (N_2) bath gas. At temperatures above 298 K no reaction of Br with MVK was observed. The only other published gas kinetic study, which used a relative rate technique to evaluate Br + MVK rate coefficients, was conducted by Sauer et al. *[1999]* at 301 ± 3 K in 1 atm synthetic air. The Sauer et al. rate coefficients showed an O_2 partial pressure dependence because their approach

observed the net effect of not only reactions (1) and (-1), but also the following reaction:

$$CH_3C(O)CHCH_2\text{-}Br + O_2 + M \leftrightarrow CH_3C(O)CH(O_2)CH_2\text{-}Br + M \qquad (I)$$

The addition reaction (I) competes with reactions (-1) for removal of $CH_3C(O)CH(O_2)CH_2$-Br, which is also, presumably what happens in the atmosphere. This study is the first to determine elementary rate coefficients for reactions (1) and (-1). We show that the results of Sauer et al. *[1999]* can be reproduced using our new kinetics results in conjunction with a reasonable estimate for k_I, thus providing needed confirmation that the assumed three-step reaction sequence is correct and the results of Sauer et al. *[1999]* are reasonable.

The reaction of Cl + MVK was studied over the temperature and pressure ranges 210 K < T < 760 K and 10 ≤ P ≤ 600 Torr in nitrogen (N_2) bath gas. Four gas kinetics studies of the Cl + MVK reaction are reported in the literature *[*Canosa-Mas et al., *1999 and 2001*, Finlayson-Pitts et al., *1999*, Orlando et al., *2003]*. Canosa-Mas et al. *[1999]*, Finlayson-Pitts et al. *[1999]*, and Orlando et al. *[2003]* all carried out relative rate studies and have only studied the reaction at room temperature and atmospheric pressure, while Canosa-Mas et al. *[2001]* investigated the reaction using the

absolute technique of discharge flow at room temperature in 1.6 and 4.5 Torr of He and N_2, respectively.

Equilibrium constants obtained from measurements of k_i and k_{-i} (i = 1,2) are used to obtain bond strengths for Br and Cl adducts with MVK. These bond strengths are compared with other known bond strengths for Br and Cl adducts with olefins, and observed trends are discussed.

CHAPTER 2

EXPERIMENTAL TECHNIQUE

Chlorine and bromine atom kinetics were studied as a function of temperature and pressure of N_2 bath gas using the laser flash photolysis – resonance fluorescence (LFP-RF) technique. This technique has proven to be an effective spectroscopic tool for kinetics studies of elementary radical-molecule reactions. Flash photolysis – resonance fluorescence was developed by Braun and co-workers *[Braun et al., 1967]* and has shown increased sensitivity and refinement with improvements in laser and signal processing technology. A schematic diagram of our LFP-RF apparatus is shown in Figure 1.

For experiments at T < 365 K, a jacketed Pyrex reaction cell with an internal volume of approximately 150 cm^3 was maintained at a constant temperature by circulating ethylene glycol (for T > 298 K) or a 2:1 ethanol-methanol mixture (T < 298 K) from a thermostated bath through the outer jacket. A copper-constantan thermocouple was inserted into the reaction vessel through a vacuum seal, thus allowing measurement of the

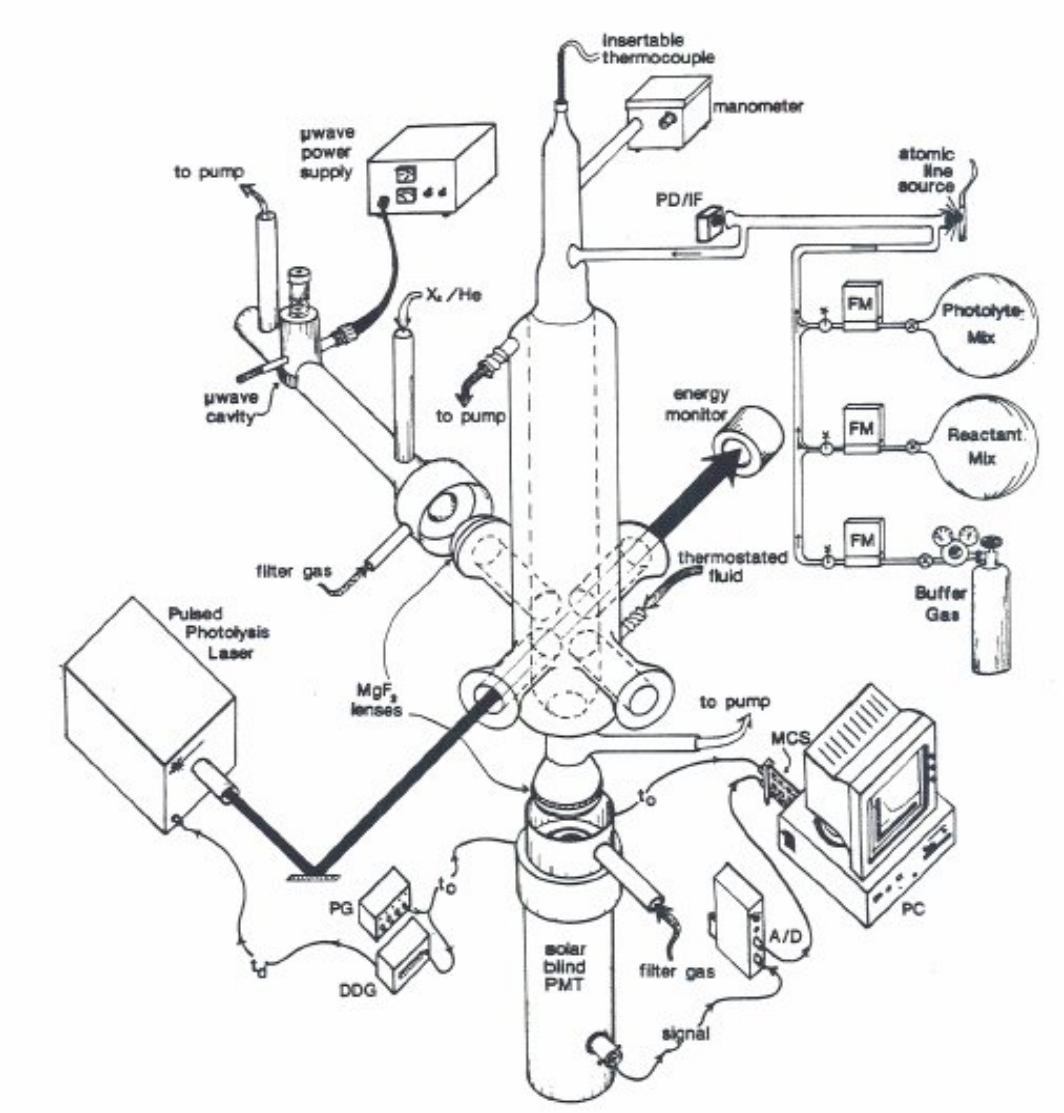

Figure 1. Schematic diagram of our Laser Flash Photolysis – Resonance Fluorescence (LFP-RF) apparatus *[Finlayson-Pitts et al., 2000]*

A/D: amplifier/discriminator; DDG: digital delay generator; FM: mass flow meter; MCS: multichannel scalar; PD/IF: photodetector/interference filter; PG: pulse generator; PMT: photomultiplier tube.

gas temperature under the precise pressure and flow rate conditions of each experiment. Temperature measurements were recorded with the thermocouple inserted into the middle of the reaction zone. The temperature variation in the reaction zone, i.e. the volume from which resonance fluorescence could be detected, was less than 2 K.

For experiments at T > 405 K, an all quartz reaction cell with an internal volume of approximately 200 cm^3 was resistively heated by using electrically insulated nichrome wire windings wrapped around the outer surface. The heated wiring was covered with ceramic felt and layers of stainless-steel radiation shields. Air-cooled jackets on the arms of the reaction cell allowed the O-ring joints to be kept near 298 K. The temperature of the gas mixture inside the reaction zone was measured using a chromel-alumel thermocouple inserted through a vacuum seal. The temperature gradient between in the top and bottom of the reaction zone (~1.5cm) was approximately ±5 K and was found not to be a significant source of uncertainty.

In each of these experiments, Br or Cl radicals were produced by either 248 nm or 266 nm laser flash photolysis of a suitable precursor (CF_2Br_2 for Br generation or $COCl_2$ for Cl generation):

$$CF_2Br_2 + h\nu(248\ nm) \rightarrow CF_2Br + Br(^2P_J) \qquad (4)$$

$Cl_2CO + h\nu(248\ nm) \rightarrow CO + 2Cl(^2P_J)$ (5)

$Cl_2CO + h\nu(266\ nm) \rightarrow CO + 2Cl(^2P_J)$ (6)

Radiation from a GAM EX50 KrF Excimer laser provided the 248 nm photolysis source. The pulse width was approximately 20 ns and fluences employed were in the range 1 - 11 mJ cm^{-2} $pulse^{-1}$. Fourth harmonic radiation from a Quanta Ray Model DCR-3 Nd:YAG laser served as the 266 nm light source; its pulse width was 6 ns and the fluences employed were in the range 3 – 12 mJ cm^{-2} $pulse^{-1}$.

An atomic resonance lamp situated perpendicular to the photolysis laser excited fluorescence in the Br or Cl atoms. Approximately 1 Torr of helium containing trace amounts of Br_2 for Br + MVK experiments or trace amounts of Cl_2 for Cl + MVK experiments was flowed from a 22-Liter glass bulb and a high pressure tank of helium. The flow rates of Br_2/He and pure He (or Cl_2/He and pure He) were controlled by separate needle valves which could be adjusted to optimize the signal-to-noise ratio. These species flowed into and were pumped out of the lamp through the two side arms. Radiation was coupled into the reaction cell through a magnesium fluoride lens. The region between the resonance lamp and the reaction cell was purged with N_2 to allow transmission of Br resonance lines in the 140 – 160 nm range or the Cl resonance lines in the 135 – 140

nm range. A few Br + MVK experiments employed 5 percent methane in N_2 as the purge gas in order to filter out impurity emissions from excited oxygen and hydrogen at wavelengths shorter than 140 nm. No significant difference in observed fluorescence temporal profiles was detected as a function of choice of purge gas. Fluorescence intensities were found to vary linearly with atom concentration up to several times higher than any employed in these kinetics experiments.

Fluorescence was collected by either a magnesium fluoride lens in the case of Br experiments or a calcium fluoride lens for Cl experiments on an axis orthogonal to both the photolysis laser beam and the resonance lamp. Fluorescence was then imaged onto the photocathode of a solar blind photomultiplier tube. The region between the reaction cell and the photomultiplier was purged with N_2. Signals were processed using photon counting techniques in conjunction with multichannel scaling. The multichannel scaler was set to collect signal before the laser fired in order to establish a pre-trigger background signal level. For each Br or Cl atom decay temporal profile measured, signals from a large number of laser shots were averaged.

In order to avoid accumulation of photochemically generated reactive species, all experiments were carried out under "slow flow"

conditions. The linear flow rate through the reaction cell ranged from 3 to 5 cm s^{-1} while the laser repetition rate was 2 - 5 Hz. The direction of flow was perpendicular to the laser beam, so no volume element of the reaction mixture was subjected to more than a few laser shots. Difluorobromomethane (CF_2Br_2) or phosgene (Cl_2CO) and methylvinyl ketone were introduced into the reaction cell from 12-L Pyrex bulbs containing diluted mixtures in N_2, while pure N_2 and CO_2 were flowed from high pressure liquid tanks. All flows into the reaction cell were controlled by calibrated mass flow meters. The CF_2Br_2/N_2 or Cl_2CO/N_2, CO_2, and additional N_2 were premixed before entering the cell. Concentrations of each component in the reaction mixture were determined from the corresponding bulb concentrations, the mass flow rates, and the total pressures. The bulb concentration of the ketone was measured frequently by UV photometry at 326 nm using a cadmium penray lamp as the light source and a 201.3 cm path length. The absorption cross section employed to determine the bulb concentration was 7.02 x 10^{-20} cm^2 $molecule^{-1}$ *[*Gierczak et al., 1997*]*.

The gases and liquid materials used in this study were: N_2 (UHP, Air Gas), He (UHP, Air Gas), CO_2 (99.99%, Air Gas), $CH_3C(O)CH=CH_2$ (99%, Aldrich), Br_2 (99%, Aldrich), CF_2Br_2 (97%, Aldrich), Cl_2 (99.9%, Spectra Gases), Cl_2CO (99.0%, Matheson Trigas). For Cl_2CO and CO_2, the stated

purity refers to the liquid phase in the high pressure gas cylinder. For Br_2, $CH_3C(O)CH=CH_2$, and CF_2Br_2, the stated purities refer to liquid samples. N_2 and He were used as supplied while all other gases and liquids were degassed repeatedly using liquid N_2 at 77 K, then diluted with gaseous N_2 and stored in 12-L Pyrex bulbs.

CHAPTER 3

RESULTS AND DISCUSSION OF Br + $CH_3C(O)CH=CH_2$ EXPERIMENTS

The reaction Br + $CH_3C(O)CH=CH_2$ + N_2 ↔ $CH_3C(O)CHCH_2$-Br + N_2 was studied under pseudo-first order conditions with $CH_3C(O)CH=CH_2$ and CF_2Br_2 in large excess over Br atoms. Both excited spin-orbit state Br atoms ($^2P_{1/2}$) and ground state atoms ($^2P_{3/2}$) are produced by the ultraviolet photo-dissociation of difluorobromomethane. The rate coefficient for quenching of Br($^2P_{1/2}$) by N_2 is (1.4 ± 0.07) x 10^{-14} cm^3 $molecule^{-1}$ s^{-1} *[Johnson et al., 1996]*. Therefore, equilibration of the spin-orbit states occurs on a time scale that is short compared to the time scale for chemical reactions under a majority of the experimental conditions employed. As an additional check on this assumption, a few experiments were carried out with approximately 1 Torr of CO_2, a very efficient Br($^2P_{1/2}$) quencher which has a known rate coefficient of 1.5 x 10^{-11} cm^3 $molecule^{-1}$ s^{-1} *[Petersen et al., 1975]*, added to the reaction mixture. As expected, the addition of CO_2 to the reaction mixture had no measurable effect on the observed kinetics. The Boltzmann equilibrium concentration of excited ($^2P_{1/2}$) is only ~6 x 10^{-9}% at 240 K and ~8 x 10^{-11}%

at 200K. Therefore, all observed kinetics are representative of ground state Br($^2P_{3/2}$) atoms.

3.1 Kinetics at 200 K < T < 250 K

In preliminary experiments, it was demonstrated that variations in laser photon fluence and photolyte concentration did not effect the observed kinetics; this suggests that secondary radical-radical and radical-photolyte reactions did not effect the observed Br temporal profiles. However, variations in temperature, pressure, and MVK concentration did show an effect on the Br temporal profiles over the temperature and pressure ranges 200 K < T < 250 K and 25 ≤ P ≤ 100 Torr. At temperatures above 298 K no reaction of Br with $CH_3C(O)CH=CH_2$ was observed which suggests that the $CH_3C(O)CHCH_2$-Br adduct is too short lived to be observed under these experimental conditions. Furthermore, no hydrogen abstraction reaction was observed up to the maximum temperature that could be investigated (~ 750 K).

Over the temperature range 200 K < T < 250 K, Br atom regeneration via a secondary reaction became evident in a manner expected if adduct formation and dissociation were controlling Br kinetics. Assuming

that $CH_3C(O)CHCH_2$-Br decomposition is the source of regenerated Br, the relevant kinetic scheme controlling Br temporal profiles includes reactions 1, -1, and the following:

Br → first-order loss by diffusion from the detector field of view and/or reaction with background impurities (7)

$CH_3C(O)CHCH_2$-Br → first-order loss by processes that do not regenerate Br (8)

The background Br atom loss rate (k_7) was directly measured at each temperature and pressure. The rate equations for reactions 1, -1, 7, and 8 can be solved analytically to yield the following:

$$S_t/S_0 = \{(Q + \lambda_1) \exp(\lambda_1 t) - (Q + \lambda_2) \exp(\lambda_2 t)\}/(\lambda_1 - \lambda_2) \quad \text{(II)}$$

where S_t and S_0 are the resonance fluorescence signal levels at times t and 0, and the fit parameters Q, λ_1, and λ_2 are related to the elementary rate coefficients as follows:

$$Q = k_{-1} + k_8 \quad \text{(III)}$$

$$Q + k_7 + k_1[MVK] = -(\lambda_1 + \lambda_2) \quad \text{(IV)}$$

$$k_7 Q + k_8 k_1[MVK] = \lambda_1 \lambda_2 \quad \text{(V)}$$

The observed Br temporal profiles were fit to the double exponential equation (II) using a nonlinear least-squares technique to obtain values of S_0, Q, λ_1, and λ_2. Rearrangement of equations (II - V) gives relationships for the rate coefficients k_1, k_{-1}, and k_8 as follows:

$$k_1 = -(Q + k_7 + \lambda_1 + \lambda_2)/[MVK] \quad \text{(VI)}$$

$$k_8 = (\lambda_1\lambda_2 - k_7Q)/k_1[MVK] \quad \text{(VII)}$$

$$k_{-1} = Q - k_8 \quad \text{(VIII)}$$

Typical experimental Br temporal profiles observed over 200 K < T < 250 K temperature range are shown in Figure 2. All experimental results are summarized in Table 1. Values for the equilibrium constant (K_P) are given in Table 1 and are derived from the following relationship:

$$K_P = k_1/(k_{-1}RT) = K_C/(RT) \quad \text{(IX)}$$

The results at 222 K, the midpoint of the experimental T^{-1} range, show that k_1 and k_{-1} have strong pressure dependencies while K_P shows very little, as expected for a reversible addition reaction. These observations add confidence that the non-linear least squares fitting procedure is relatively free of systematic errors.

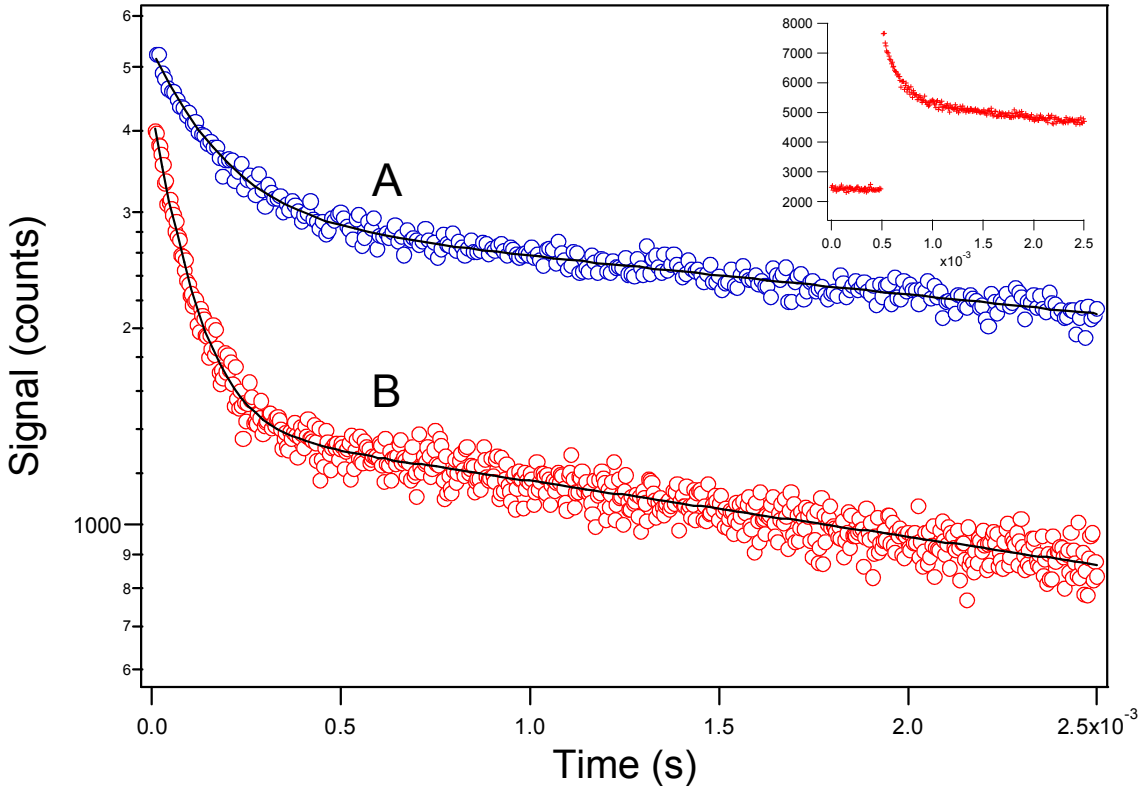

Figure 2. Typical Br atom temporal profiles observed in this study

Experimental Conditions**:** T = 233 K; P = 100 Torr; $[CF_2Br_2]$ = 3.4 × 10^{13} molecule cm^{-3}; $[Br]_{t=0}$ = 1.0 × 10^{11} atoms cm^{-3}; [MVK] in units of 10^{14} molecules cm^{-3} = (A) 1.5 (B) 3.9. Solid lines are obtained from non-linear least squares analyses. The smaller plot shows trace (B) with a pre-trigger baseline.

Table 1. Results for the Br + $CH_3C(O)CH=CH_2$ + N_2 ↔ $CH_3C(O)CHCH_2$-Br + N_2

T	P	$[CF_2Br_2]$	[Br]	[MVK]	S_0	Q	λ_1	λ_2	k_1	k_{-1}	k_7	k_8	K_p
203	100	42.5	0.058	31.5	2290	441	-1320	-235	3.52	180	45	261	709
203	100	42.1	0.060	87.0	2970	710	-3710	-445	3.96	240	45	470	597
203	100	41.6	0.063	140	2380	965	-6180	-579	4.13	355	45	610	422
203	100	41.5	0.060	249	2080	2140	-11700	-1420	4.42	632	45	1507	254
212	26	43.3	0.048	97.4	2720	646	-2270	-231	1.91	374	15	272	176
212	26	43.9	0.051	101	2870	652	-2290	-242	1.86	368	30	284	175
212	25	44.1	0.051	407	2270	1040	-6920	-584	1.59	423	30	621	130
212	25	44.2	0.050	415	2250	737	-6770	-346	1.54	374	15	364	142
217	25	40.6	0.14	217	9760	775	-3920	-233	1.56	509	21	266	103
217	25	41.2	0.14	419	7450	796	-6100	-277	1.33	496	21	299	90.5
217	25	41.9	0.15	425	5690	1120	-6170	-493	1.31	572	21	545	77.1
217	25	40.4	0.14	757	5350	1190	-11000	-506	1.37	649	21	536	71.2
217	25	42.0	0.15	767	3710	1380	-11000	-634	1.34	702	21	677	64.4
219	100	36.3	0.11	58.8	7210	1250	-2820	-190	2.98	965	26	286	104
219	100	36.2	0.11	211	8180	1220	-6320	-215	2.53	968	26	249	87.4
219	100	35.4	0.11	397	5020	1410	-11500	-274	2.61	1112	26	300	78.4
219	100	36.5	0.12	707	3610	1740	-19800	-436	2.62	1272	26	465	68.8
220	200	36.0	0.061	56.8	3370	1070	-3240	-206	4.19	800	30	267	175
220	200	36.7	0.063	392	2400	1610	-16200	-487	3.85	1091	30	520	118
220	200	39.4	0.067	208	2950	1130	-8620	-260	3.72	844	30	284	147
220	200	36.7	0.063	392	2400	1610	-16200	-487	3.85	1091	30	520	118
226	25	40.6	0.15	133	9620	1150	-2670	-153	1.26	924	23	229	44.4
226	25	37.4	0.14	392	5600	1240	-5640	-207	1.17	994	23	248	38.4
226	25	19.2	0.070	418	2860	1260	-6090	-203	1.20	1019	23	239	38.5
226	25	9.5	0.035	421	1870	1210	-5930	-171	1.16	1007	23	202	37.6
226	25	38.0	0.14	731	6380	1350	-9620	-274	1.17	1041	23	305	36.6

Units: T (K); P (Torr); concentrations (10^{12} molecules cm^{-3}); k_{-1}, k_7, k_8 (s^{-1}); k_1 (10^{-11} cm^3 $molecule^{-1}$ s^{-1}); K_P ($10^4 atm^{-1}$)

Table 1. (continued)

T	P	$[CF_2Br_2]$	[Br]	[MVK]	S_0	Q	λ_1	λ_2	k_1	k_{-1}	k_7	k_8	K_p
228	100	36.5	0.12	47.6	10900	2030	-2990	-110	2.24	1769	24	263	40.9
228	100	36.6	0.12	220	1000	2010	-6020	-176	1.90	1769	24	242	34.7
228	100	8.9	0.03	367	4900	2160	-9660	-154	2.08	1971	24	188	34.1
228	100	35.9	0.13	402	7600	2140	-9860	-199	1.97	1897	24	242	33.5
228	100	35.3	0.13	726	5780	2370	-16700	-289	2.02	2042	24	326	31.9
231	25	39.3	0.12	114	5970	1670	-2410	-116	0.751	1385	21	285	17.2
231	25	38.9	0.12	314	5600	1810	-4350	-175	0.865	1542	21	266	17.8
231	25	39.6	0.12	435	4190	2050	-5820	-284	0.932	1653	21	397	17.9
231	25	39.2	0.12	830	3050	2200	-9780	-315	0.952	1813	21	385	16.7
233	100	33.9	0.095	151	5320	3400	-6040	-136	1.83	3143	29	261	18.3
233	100	34.8	0.10	392	4350	3790	-11200	-197	1.93	3509	29	276	17.4
233	100	34.2	0.099	708	3770	3890	-17500	-234	1.96	3603	29	287	17.1
233	100	34.6	0.10	985	3140	4040	-24000	-270	2.05	3721	29	315	17.4
238	25	38.9	0.10	407	3270	3280	-6490	-219	0.842	2889	22	395	9.00
238	25	38.2	0.097	767	2510	3610	-10400	-278	0.925	3214	22	397	8.89
238	25	38.8	0.10	1130	2610	3420	-12600	-298	0.841	3028	22	389	8.57
239	100	35.5	0.087	526	3460	6220	-14700	-192	1.66	5914	25	307	8.60
239	100	33.7	0.080	708	2210	6460	-18600	-202	1.74	6166	25	292	8.66
239	100	34.3	0.082	1020	2650	6680	-24800	-245	1.81	6355	25	322	8.75
239	100	34.7	0.085	1310	2760	6790	-29300	-268	1.74	6456	25	337	8.26
241	25	35.6	0.068	888	2760	4150	-11500	-252	0.850	3782	23	370	6.84
241	25	33.4	0.061	1030	2720	4020	-11900	-258	0.787	3651	23	366	6.56
241	25	33.8	0.062	1370	3080	4230	-15300	-273	0.830	3867	23	360	6.53

Units: T (K); P (Torr); concentrations (10^{12} molecules cm^{-3}); k_{-1}, k_7, k_8 (s^{-1}); k_1 (10^{-11} cm^3 $molecule^{-1}$ s^{-1}); K_P ($10^4 atm^{-1}$)

3.2 $CH_3C(O)CHCH_2$-Br Thermochemistry: Second-Law Analysis

The equilibrium constants, K_P, given in Table 1 can be used to obtain information about the thermochemistry of the Br + $CH_3C(O)CH=CH_2 \leftrightarrow CH_3C(O)CHCH_2$-Br reaction using the following relationship:

$$\ln(K_P) = (\Delta_rS/R) - (\Delta_rH/RT) \qquad (X)$$

A van't Hoff plot of $\ln(K_P)$ vs versus T^{-1} is shown in Figure 3. The enthalpy change associated with reaction (1) is obtained from the slope of the van't Hoff plot while the entropy change is obtained from the intercept. At 222 K, this 'second-law analysis' gives the results $\Delta_rH = -10.9 \pm 0.3$ kcal mol^{-1} and $\Delta_rS = -23.0 \pm 1.3$ cal mol^{-1} K^{-1} where the errors are 2σ and represent precision only.

3.3 $CH_3C(O)CHCH_2$-Br Thermochemistry: Third-Law Analysis

In addition to the second-law analysis, a third law analysis was carried out, where the experimental value for K_P at 222 K, $(5.6 \pm 1.4) \times 10^5$ atm^{-1}, was employed in conjunction with a calculated entropy change to determine Δ_rH at 222 K for reaction (-1) using equation (X).

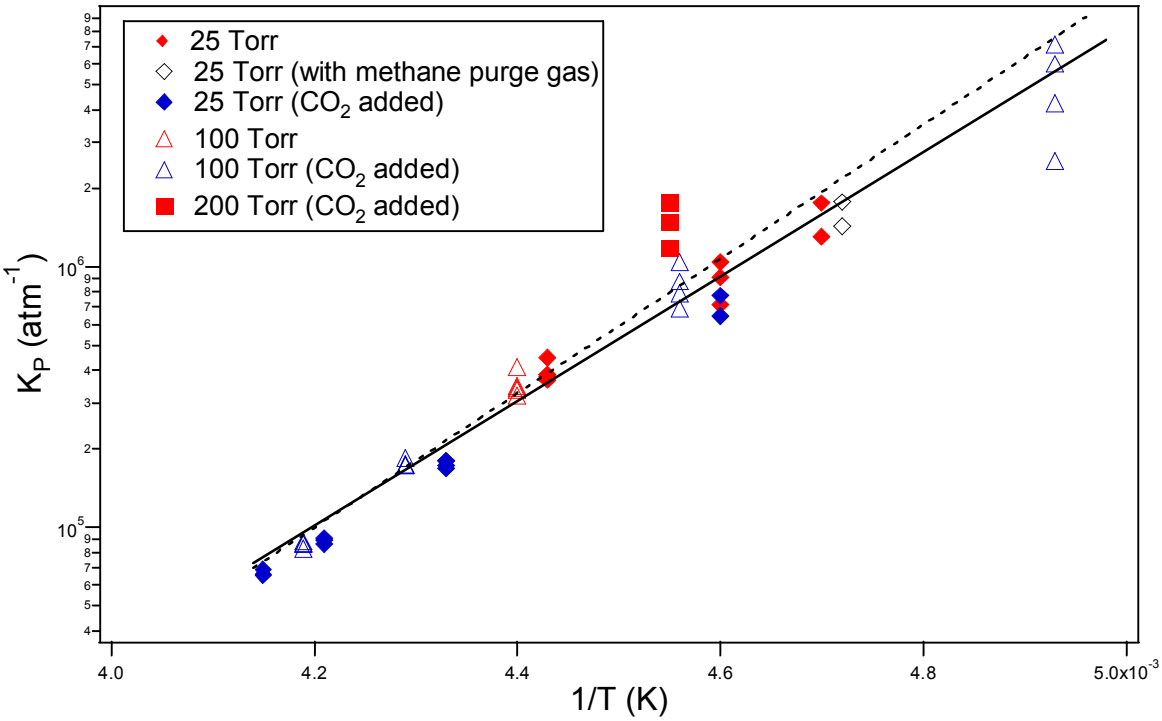

Figure 3. Van't Hoff Plot for the Br + $CH_3C(O)CH=CH_2$ ↔ $CH_3C(O)CHCH_2$-Br equilibrium

The solid line is obtained from a least squares analysis of K_P versus T^{-1} and gives the second-law thermochemical parameters for the reaction. The dashed line shows the third-law thermochemical parameters for the reaction. Different symbol shapes indicate data obtained at different pressures.

Only one type of $CH_3C(O)CHCH_2$-Br adduct is believed to be formed. Theoretical calculations, carried out by our collaborator M.L. McKee of Auburn University, predict the bromine atom adds to the terminal carbon on the double bond to form a 2-center – 2-electron bond. The calculated structure for the $CH_3C(O)CHCH_2$-Br adduct is shown in Figure 4. As shown in Figure 4, the most stable adduct is one where Br adds to the internal carbon of the double bond. However, this adduct cannot form in our study because of the large barrier to addition at the internal carbon site. For comparison, the calculated energetics at a higher level of theory than in Figure 4 (CCSD(T)/6-311+g(2d,p)/Br(SDD)//B3LYP/6-31+G(d)/ Br(SDD)+ZPC) yielded an enthalpy change at 0 K of −11.87 kcal mol^{-1} as summarized in Table 3.

To determine Δ_rS for reaction (-1), absolute entropies as a function of temperature were obtained from the JANAF tables *[Chase et al., 1985]* for Br and calculated using *ab initio* vibrational frequencies and moments of inertia for $CH_3C(O)CHCH_2$ and the $CH_3C(O)CHCH_2$-Br adduct obtained from McKee's calculations (see above). Important parameters used in calculations of absolute entropies and heat capacity corrections are summarized in Table 2. At 222 K, the third law analysis gives Δ_rH = −11.8 ± 0.7 kcal mol^{-1} and Δ_rS = −26.7 ± 1.6 cal mol^{-1} K^{-1}; the uncertainties reported

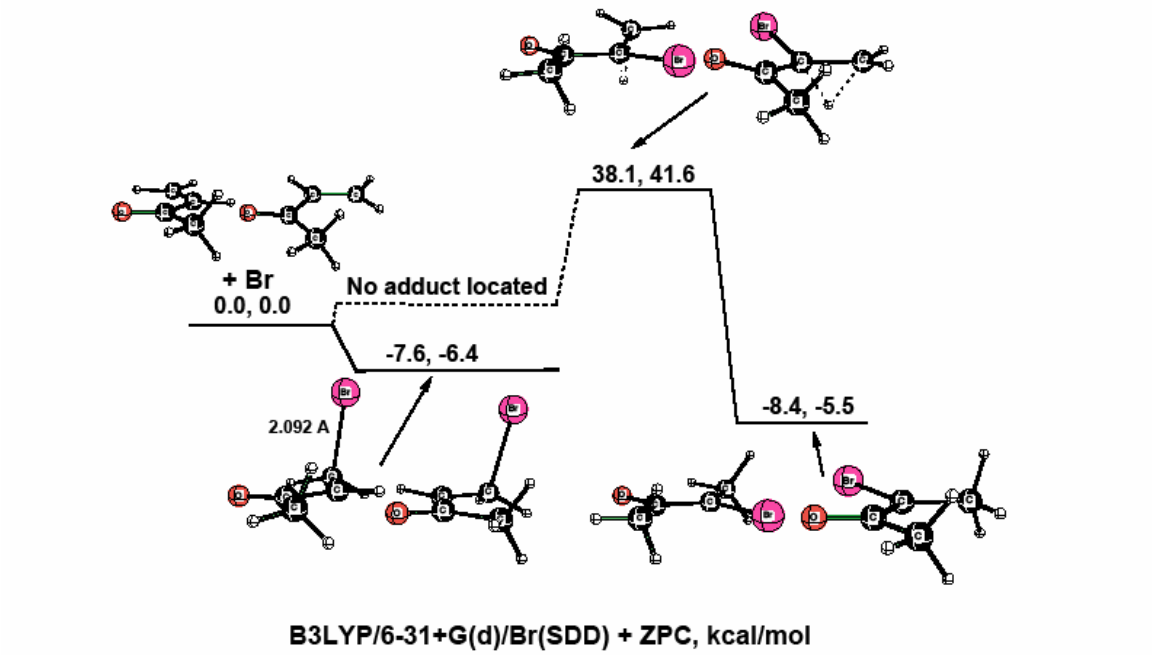

Figure 4. Structure for $CH_3C(O)CHCH_2$-Br provided by Mike McKee of Auburn University from *ab initio* calculations showing Br addition to the terminal carbon on the double bond *[McKee, 2008]*

$CH_3C(O)CHCH_2$-Br vibrations) as well as the uncertainty in experimental value for K_P at 222 K represent an estimate of the imperfect knowledge of the input data needed to calculate absolute entropies (particularly the low-frequency vibrations of the adduct).

Heat capacity corrections have been employed to determine $\Delta_rH°$ values at 298 K and 0 K; results are given in Table 3. The thermochemical parameters determined by the second and third-law analyses are in excellent agreement as compared in Table 3. Uncertainties listed in Table 3 are accuracy estimates at the 95% confidence level. The values for $\Delta_rH°$ can be used in conjunction with literature values for standard enthalpies of formation of Br *[Chase et al., 1985]* and MVK *[Guthrie, 1978]* to deduce values for the standard enthalpy of formation of $CH_3C(O)CHCH_2$-Br, also given in Table 3.

3.4 Literature Comparison

In 1999, Sauer et al. *[1999]* studied the gas-phase reaction of Br radicals with methylvinyl ketone using a relative kinetic technique in 1atm synthetic air at 301 ± 3 K. The rate coefficient obtained for the reaction was (1.87 ± 0.06) x 10^{-11} cm^3 $molecule^{-1}$ s^{-1}. Sauer et al. *[1999]* represents the only other gas kinetic study of the Br + $CH_3C(O)CH=CH_2$ reaction.

Table 2. Summary of parameters used in calculations of absolute entropies and heat capacity corrections for the Br + $CH_3C(O)CH=CH_2$ ↔ $CH_3C(O)CHCH_2$-Br reaction

	Br	**$CH_3C(O)CH=CH_2$**	**$CH_3C(O)CHCH_2$-Br**
g_0	4	1	2
g_1	2		
$\Delta\varepsilon/cm^{-1}$ [a]	3685.24		
σ		2	2
Rot. Constants/cm^{-1} [b]		0.296, 0.147, 0.0973	0.200, 0.0298, 0.0292
Vib. Frequencies/cm^{-1} [b]		110, 124, 276, 431, 491, 536, 697, 766, 955, 987, 1037, 1057, 1080, 1282, 1317, 1411, 1459, 1495, 1501, 1690, 1753, 3052, 3110, 3163, 3167, 3187, 3247	60, 63, 79, 239, 251, 415, 431, 524, 593, 727, 788, 948, 982, 1040, 1113, 1167, 1191, 1236, 1408, 1429, 1487, 1496, 1498, 1648, 3046, 3103, 3154, 3162, 3197, 3239

[a] $\Delta\varepsilon$ ≡ energy splitting between the lowest two electronic states; both $CH_3C(O)CH=CH_2$ and $CH_3C(O)CHCH_2$-Br are assumed to have no energetically accessible excited electronic states.

[b] Calculated values at the B3LYP/6-31+G(d)/ Br(SDD)+ZPC level of theory.

Table 3. Thermochemical parameters for the reaction Br + $CH_3C(O)CH=CH_2 \leftrightarrow CH_3C(O)CHCH_2$-Br

T	Method	$-\Delta_rH$	$-\Delta_rS$
298	2nd law	11.0 ± 0.3	23.1 ± 1.3
	3rd law	11.8 ± 0.7	26.8 ± 2.2
222	2nd law	10.9 ± 0.3	23.0 ± 1.3
	3rd law	11.8 ± 0.7	26.7 ± 2.1
0	2nd law	10.6 ± 0.3	
	3rd law	11.4 ± 0.7	
	B3LYP/6-31+G(d)/ Br(SDD)+ZPC (anti conformer)	7.6	
	CCSD(T)/6-311+g(2d,p)/Br(SDD)/ /B3LYP/6-31+G(d)/ Br(SDD)+ZPC (anti conformer)	11.87	
$\Delta H_{f,298}$ ($CH_3C(O)CHCH_2$-Br) = 42.8 ± 2.7			

Units: T (K); P (Torr); Δ_rH, $\Delta H_{f,T}$ (kcal mol^{-1}); Δ_rS (cal mol^{-1} K^{-1})

Importantly however, for Br reactions to double bonds, temperature and partial pressure variations of O_2 are known to affect observed kinetics *[Barnes et al., 1989, Ramacher et al., 2000]*. Extra experiments by Sauer et al. *[1999]* were conducted as a function of O_2 partial pressure which indeed yielded an O_2 dependence. Therefore, the rate coefficient obtained by Sauer et al. *[1999]* was the net of three different reactions obtained at one temperature and total pressure, i.e., reactions (1), (-1), and the additional reaction:

$CH_3C(O)CHCH_2$-Br + O_2 + M $\leftrightarrow$ $CH_3C(O)CH(O_2)CH_2$-Br + M (I)

The results from Sauer et al. *[1999]* cannot readily be extrapolated to other temperature and pressure conditions. However, rate coefficients for the Br + MVK association and adduct dissociation reactions reported in this study can be used to test the reasonableness of Sauer et al.'s results and also to provide a basis for extrapolation to lower temperatures that are of atmospheric interest. Extrapolating the plot in Figure 3 to 301 K gives the equilibrium constant $K_C = 3.5 \times 10^{-17}$ cm^3 molecule^{-1}. Assuming a (typical) small negative activation energy for Br addition to MVK, i.e., k = A exp(+200/T), and extrapolating our pressure dependent kinetic data (Table 1) to atmospheric pressure, we estimate that under the conditions of the Sauer et al. *[1999]* experiment, $k_1 \sim 5.5 \times 10^{-11}$ cm^3 molecule^{-1} s^{-1}. Hence, the fraction of adduct molecules that react with O_2 at 301 K and 1 atm air can be estimated based on the combined results of both studies to be ~1/3, with the other 2/3 being lost via unimolecular decomposition with a first order rate coefficient given by $k_{-1} = k_1/K_C = 1.4 \times 10^6$ s^{-1}. Hence, the pseudo-first order rate coefficient for the reaction of $CH_3C(O)\dot{C}HCH_2Br$ with O_2 is approximately $k_{-1}/2 = 7 \times 10^5$ s^{-1}, which implies a bimolecular rate coefficient for the $CH_3C(O)\dot{C}HCH_2Br + O_2$ reaction (k_I) of 1.4×10^{-13} cm^3 molecule^{-1} s^{-1} at T = 301 ± 3 K and P = 1 atm synthetic air; this is a reasonable value for k_I. Based on the temperature dependence of k_{-1} determined in this study and the expectation that k_I will have little or no

temperature dependence, it is clear that at low temperatures typical of those where polar ozone depletion events are observed, essentially all adduct molecules will react with O_2 before dissociating and the overall rate coefficient for loss of MVK by reaction with Br will be equal to k_1.

In addition to their relative rate measurements, Sauer et al. *[1999]* conducted product studies at (900 ± 20) mbar synthetic air and (296 ± 3) K using FT-IR spectroscopy. This technique allowed in situ measurement of both the reactants and products. The study stated both terminal and non-terminal addition accounted for (92 ± 15)% of the total reaction with the yield of terminal addition product(s) being three times larger than the yield of non-terminal addition product(s). As seen from the theoretical structure at the B3LYP/6-31+G(d)/ Br(SDD)+ZPC level of theory in Figure 4 *[*McKee, 2008*]*, the experimental calculations also predict that terminal addition is the dominant pathway.

Bond strengths for some other adducts of Br to olefins have been studied and can be compared to the Br + MVK case. Bedjanian et al. *[1998, 1999, 2000]* conducted discharge flow studies between 233 and 320 K in 0.5 – 2.0 Torr He for several Br + alkene reactions. First, Bedjanian et al. *[1998]* studied the reaction Br + propene (C_3H_6) and obtained Δ_rH = –(7.7 ± 1.4) kcal mol^{-1}at 298 K. Secondly, Bedjanian et al. *[1999]* studied the separate reactions Br + ethene (C_2H_4) and trans-2-butene (C_4H_8) and

obtained Δ_rH = –(6.8 ± 1.6) kcal mol^{-1} and Δ_rH = –(8.8 ± 1.5)kcal mol^{-1}, respectively at 298 K. For comparison, an LFP-RF study was carried out by Ferrell *[1998]* in our lab for the Br + ethene reaction which determined Δ_rH = –(7.1 ± 0.53) kcal mol^{-1}at 298 K. Third, Bedjanian et al. *[2000]* studied the separate reactions Br + 2-methyl-2-butene (C_5H_{10}) and 2,3-dimethyl-2-butene (C_6H_{12}) and obtained Δ_rH = –(10.0 ± 1.6) kcal mol^{-1} and Δ_rH = –(9.8 ± 2.4) kcal mol^{-1}, respectively at 298 K. It is worth pointing out that the studies from our lab measured the forward and reverse rate coefficients directly at atmospherically relevant pressures whereas the studies of Bedjanian et al. were restricted to pressures of a few Torr or less and obtained information about the adduct dissociation reaction only by competitive kinetics methods (relative to the adduct + Br_2 reactions). The importance of bond strength comparisons for Br + MVK to other unsaturated species are addressed in Chapter 5.

A study has been reported by Ramacher et al. *[2000]* where rate coefficients for the reactions of Br atoms with trichloroethene (C_2HCl_3), ethene, and tetrachloroethene (C_2Cl_4) have been obtained using the relative rate technique over the temperature range 228 – 298 K in 700 Torr of air. Room temperature rate coefficients obtained for C_2HCl_3 and C_2Cl_4 are (in units of cm^3 $molecule^{-1}$ s^{-1}), 1.56 x 10^{-13}, 1.23 x 10^{-13}, and <1.2 x 10^{-16}, respectively. The rate coefficients for these reactions can be directly compared with the rate coefficient obtained by Sauer et al. *[1999],*

determined at 301 ± 3 K in 1 atm synthetic air, which shows a significantly faster rate for the reaction of Br with MVK. The faster rate coefficient observed by Sauer et al. *[1999],* (1.87 ± 0.06) x 10^{-11} cm^3 $molecule^{-1}$ s^{-1}, indirectly indicates the bond strength for the MVK-Br adduct is significantly stronger than for adducts formed by reaction of Br with C_2HCl_3, C_2H_4, or C_2Cl_4.

CHAPTER 4

RESULTS AND DISCUSSION OF Cl + $CH_3C(O)CH=CH_2$ EXPERIMENTS

The reaction Cl + $CH_3C(O)CH=CH_2$ was studied under pseudo-first order conditions with $CH_3C(O)CH=CH_2$ in large excess over Cl atoms. Both excited spin-orbit state Cl atoms ($^2P_{1/2}$) and ground state atoms ($^2P_{3/2}$) are produced by the ultraviolet photo-dissociation of phosgene; the fraction of excited ($^2P_{1/2}$) has been reported to be ~15% at 235 nm *[Maul et al., 1995]*. The rate coefficients for quenching of Cl($^2P_{1/2}$) by N_2 and Cl_2CO are (in units of cm^3 $molecule^{-1}$ s^{-1}), 5.0 x 10^{-15} *[Tyndall et al., 1995]* and 3.0 x 10^{-10} *[Chichinin, 1993]*, respectively. Therefore, equilibration of the spin-orbit states occurs on a time scale that is short compared to the time scale for chemical reactions under a majority of the experimental conditions employed, and it can be safely assumed that all the data reported in this study are representative of an equilibrium mixture of Cl spin-orbit states. Additionally, most experiments were carried out with approximately 1 Torr of CO_2, a very efficient Cl($^2P_{1/2}$) quencher, added to the reaction mixture to speed up spin state equilibration. The Boltzmann equilibrium fraction of spin-orbit excited atoms is 0.04% at 200 K, 0.4% at 300 K, and 4% at 700 K.

In preliminary experiments it was demonstrated that variations in laser photon fluence and photolyte (Cl_2CO) concentration did not effect the observed kinetics; this confirms that secondary radical-radical and radical-photolyte reactions did not effect the observed Cl temporal profiles.

4.1 Kinetics at 600 K < T < 760 K

At temperatures above 600K, observed Cl temporal profiles can be described analytically by the following equation:

$$\ln\{(Cl)_0[(Cl)_t\} = (k_3[MVK] + k_9) = k't \qquad (XI)$$

where k_9 is the rate coefficient of the reaction:

$$Cl \rightarrow \text{first-order loss by diffusion from the detector field of view and/or reaction with background impurities} \qquad (9)$$

Typical Cl temporal profiles observed over this temperature range are shown in Figure 5; pseudo-first order decay rates, k', are obtained from the slopes of these plots. The bimolecular rate coefficients are obtained using linear least-squares analyses from the slopes of k' vs [MVK] plots obtained at constant temperature and pressure; typical data are shown

in Figure 6. All Cl temporal profiles at T > 600 K and P = 25 – 200 Torr were exponential, i.e. obeyed equation (XI), and the first order decay rates, k', were linearly dependent on MVK concentration and were invariant to variations in laser photon fluence and photolyte concentration. All experimental results of kinetic data for reaction (3) in this temperature range are summarized in Table 4 where the errors in the overall rate coefficients are 2σ and represent precision only.

As expected for a reaction that occurs via hydrogen abstraction as shown by reaction (3), no significant pressure dependence was observed. Additionally, over this temperature regime, k_3 was found to increase with increasing temperature. The rate coefficient, k_3, and temperatures for the reactions given in Table 4 can be used to generate an Arrhenius expression for the Cl + $CH_3C(O)CH=CH_2$ ↔ $\dot{C}H_2C(O)CH=CH_2$ + HCl reaction using the following relationship:

$$k = Aexp(–Ea/RT) \qquad (XII)$$

An Arrhenius plot of $ln(k_3)$ versus T^{-1} is shown in Figure 6. The solid line in the figure is obtained from a linear least-squares analysis and gives the following uncorrected Arrhenius expression for 600 K < T < 760 K (uncertainties are 2σ and represent precision only):

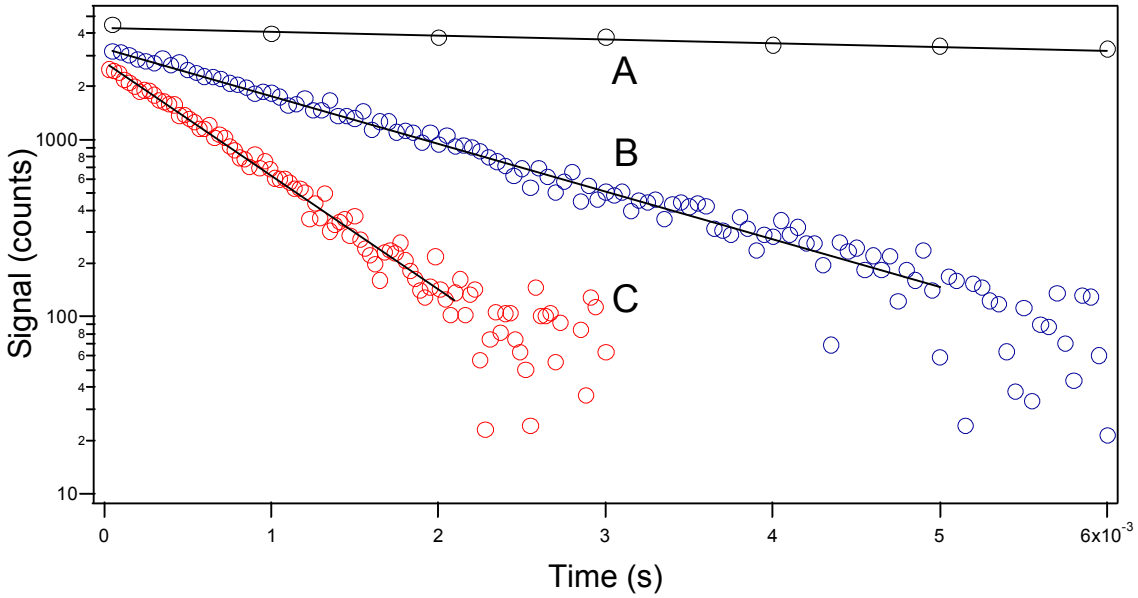

Figure 5. Typical Cl temporal profiles observed at 600 K < T < 760 K

Experimental Conditions**:** T = 755 K; P = 200 Torr; $[Cl_2CO]$ = 4.5 × 10^{14} molecule cm^{-3}; $[Cl]_{t=0}$ = 2.1 × 10^{11} atoms cm^{-3}; [MVK] in units of 10^{14} molecules cm^{-3} = (A) 0 (B) 0.86 (C) 2.2 Solid lines are obtained from linear least squares analyses. Trace B is scaled upward by 1.5 for clarity.

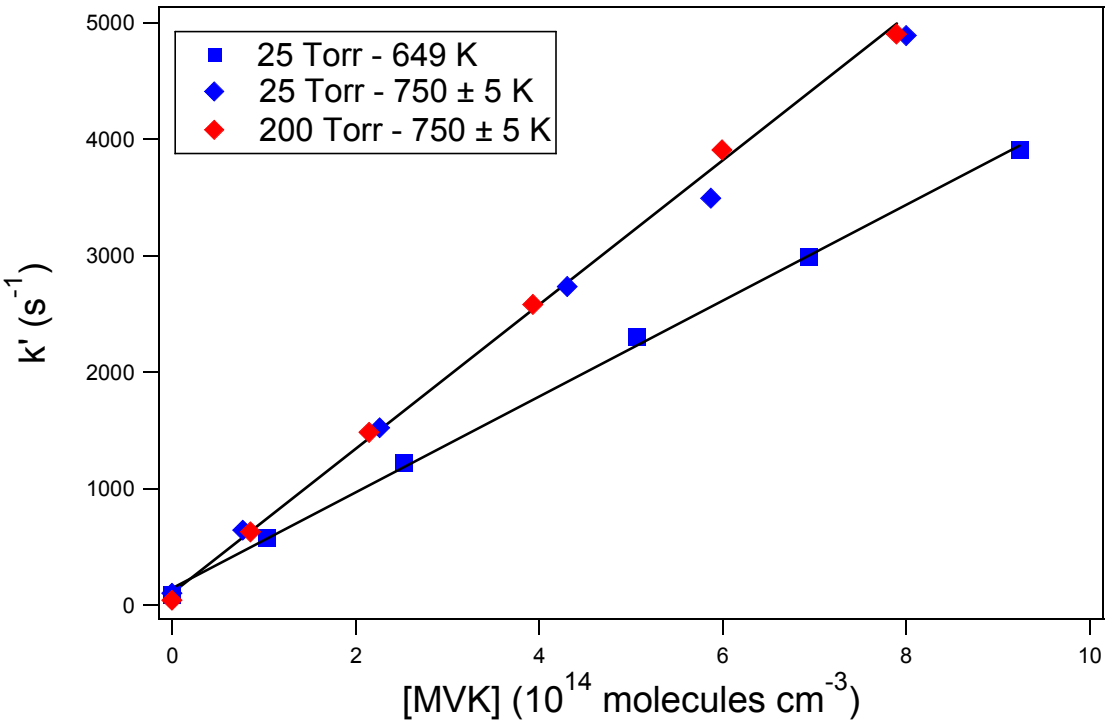

Figure 6. Plots of k' vs [MVK] for data obtained at 600 K < T < 760 K

The solid lines are obtained from linear least squares analyses.

$k_3^{uncorr}(T) = (6.94 \pm 1.13) \times 10^{-11} \exp[-(1837 \pm 84)/T]$ cm^3 molecule^{-1} s^{-1} (XIII)

The rate coefficient k_3^{uncorr} and, therefore, the Arrhenius expression, are subject to small corrections due to the occurrence of the reversible addition reaction; these corrections are discussed in section 4.4. For the sake of clarity, only the corrected rate coefficients are plotted on the Arrhenius plot in Figure 7.

4.2 Kinetics at 405 K < T < 510 K

Over the temperature 405 K < T < 510 K and pressure range 12 Torr ≤ P ≤ 200 Torr, Cl temporal profiles were effected by variations in temperature, pressure, and MVK concentration in a manner similar to that observed for Br + MVK (section 3.1), i.e., chlorine atom regeneration via a secondary reaction became evident in a manner expected if adduct formation and dissociation were controlling kinetics. Assuming that $CH_3C(O)CHCH_2$-Cl decomposition is the source of regenerated Cl, the relevant kinetic scheme controlling the Cl temporal profile includes reactions 2, -2, 9, and the following:

Table 4. Results for the Cl + $CH_3C(O)CH=CH_2 \rightarrow \dot{C}H_2C(O)CH=CH_2$ + HCl reaction at 600 K < T < 760 K

T	P	No. Expts.	$[Cl_2CO]$	[Cl]	$[MVK]_{max}$	k'_{max}	k_3^{uncorr}	k_3^{corr}
602	25	8	225	0.168	915	2967	3.23 ± 0.14	3.56 ± 0.12
649	25	6	537	0.260	923	3906	4.11 ± 0.13	< 1% difference
658	200	6	536	0.242	717	3273	4.42 ± 0.21	same as k_3^{uncorr}
702	25	11	358	0.253	857	4275	4.94 ± 0.21	"
745	25	6	400	0.224	800	4886	5.86 ± 0.21	"
755	200	6	427	0.207	799	4898	6.14 ± 0.28	"

Units: T (K); P (Torr); concentrations (10^{12} molecules cm^{-3}); k' (s^{-1}); k_3 (10^{-12} cm^3 $molecule^{-1}$ s^{-1})

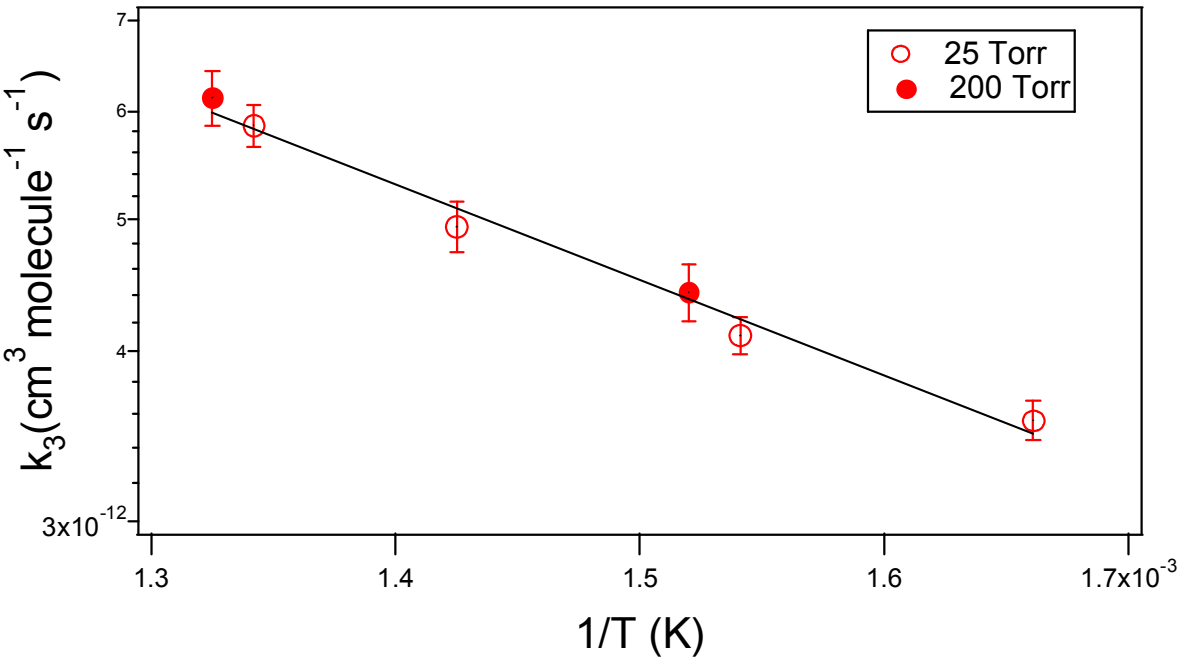

Figure 7. Corrected Arrhenius Plot Results for the Cl + $CH_3C(O)CH=CH_2 \rightarrow$ $\dot{C}H_2C(O)CH=CH_2$ + HCl reaction

$CH_3C(O)CHCH_2\text{-}Cl \rightarrow$ first-order loss by processes that do not regenerate Cl (10)

Similarly to Br, the rate equations for reactions 2, -2, 9, and 10 can be solved analytically to give Equation (II), where S_t and S_0 are the resonance fluorescence signal levels at times t and 0. The fit parameters Q, λ_1, and λ_2 are related to the elementary rate coefficients as follows:

$$Q = k_{-2} + k_{10} \quad \text{(XIV)}$$

$$Q + k_9 + (k_2 - k_3)[MVK] = -(\lambda_1 + \lambda_2) \quad \text{(XV)}$$

$$k_9Q + k_{10}(k_2 - k_3)[MVK] = \lambda_1\lambda_2 \quad \text{(XVI)}$$

The observed Cl temporal profiles were fit to the double exponential equation (I). Rearrangement of equations (II, XIV – XVI) gives relationships for the rate coefficients k_2, k_{-2}, and k_{10} as follows:

$$k_2 = -(Q + k_9 + \lambda_1 + \lambda_2)/[MVK] - k_3 \quad \text{(XVII)}$$

$$k_{10} = (\lambda_1\lambda_2 - k_9Q)/(k_2 - k_3)[MVK] \quad \text{(XVIII)}$$

$$k_{-2} = Q - k_{10} \quad \text{(XIX)}$$

The rate coefficients k_2 are subject to small corrections due to the occurrence of the H-abstraction reaction; these corrections are discussed

in section 4.4. The background Cl atom loss rate, k_9, was directly measured at each temperature and pressure.

Typical experimental Cl temporal profiles observed over this temperature range were similar to those for Br shown in Figure 2. All experimental results which include the best fits to the data are summarized in Table 5. The values for the equilibrium constant K_P are given in Table 5 and are derived from the following relationship:

$$K_P = k_2/(k_{-2}RT) = K_C/(RT) \qquad (XX)$$

The results at 465 K, the midpoint of the experimental T^{-1} range, show that k_2 and k_{-2} have strong pressure dependencies as expected for a reversible addition reaction. While K_P should, in theory, be independent of inert gas pressure, the data indicate a slight pressure dependence (see Figure 8). Possible explanations for this trend are discussed in Section 4.6.

4.3 Kinetics at 210 K < T < 365 K

Over the temperature range 210 K < T < 365 K and pressure range 10 Torr ≤ P ≤ 600 Torr, Cl temporal profiles showed exponential decay similar to those seen at 600 K < T < 760 K (Figure 5). However, Cl atom decay rates observed at short times following the laser flash were considerably faster

than those observed at T > 600 K. Also in contrast to the high-temperature experiments, for a given temperature and MVK concentration it was found that the rate of Cl loss increased with increasing N_2 pressure. These observations suggest that the dominant observed reaction pathway in the low temperature regime (< 365 K) is irreversible addition of Cl to MVK. All experimental kinetic data for reaction (2) in this temperature range are summarized in Table 6. The bimolecular rate coefficients are obtained using linear least-squares analyses from the slopes of k' vs [MVK] plots obtained at constant temperature and pressure and are similar to those shown in Figure 6. Errors in the overall rate coefficients are 2σ and represent precision only.

4.4 $CH_3C(O)CHCH_2$-Cl Corrections to Rate Coefficients

At temperatures ~600 K, reaction (-2) was too fast for the equilibrium reaction between Cl and $CH_3C(O)CHCH_2$-Cl to be directly observed with our experimental time resolution of a few microseconds. However, $CH_3C(O)CHCH_2$-Cl did represent a small Cl reservoir, and its kinetics have been taken into account.

Due to stability, $CH_3C(O)CHCH_2$-Cl does not react with MVK at the lower temperatures employed in this study. Under the assumptions: (i) $CH_3C(O)CHCH_2$-Cl is an unreactive species and (ii) equilibrium is

Table 5. Results for the Cl + $CH_3C(O)CH=CH_2$ + N_2 ↔ $CH_3C(O)CHCH_2$-Cl reaction at 405 K < T < 510 K + N_2

T	P	$[Cl_2CO]$	[Cl]	[MVK]	S_0	Q	λ_1	λ_2	k_2	k_{-2}	k_9	k_{10}	K_P
409	26	104	0.0459	0.851	3360	67	-682	-36	6.80	33	64	34	374
409	26	105	0.0464	1.46	3090	79	-1210	-45	7.50	36	64	44	378
409	26	100	0.0420	5.38	2200	64	-4360	-24	7.81	40	64	23	348
433	26	96.0	0.0415	0.800	3440	137	-600	-38	5.58	102	45	35	92.9
433	26	99.5	0.0501	1.40	2580	171	-1100	-46	6.56	127	45	44	87.8
433	26	97.6	0.0433	2.96	2500	191	-2220	-54	6.77	139	45	52	82.9
442	25	56.7	0.0295	1.87	2930	267	-1330	-41	5.20	246	104	21	35.1
442	26	57.1	0.0315	4.17	2490	317	-2810	-47	5.72	283	104	35	33.6
449	101	127	0.0542	1.20	2010	990	-1730	-57	6.42	902	15	88	11.6
449	101	122	0.0521	2.15	2050	1080	-2690	-64	7.56	1008	15	76	12.3
449	101	126	0.0524	4.77	1850	1080	-4790	-63	7.75	1017	15	59	12.5
449	101	124	0.0516	7.95	1320	1170	-7580	-69	7.99	1105	15	59	11.8
450	51	52.0	0.0102	1.18	643	657	-1500	-42	7.06	618	31	38	18.6
450	51	151	0.0282	4.98	355	662	-4050	-63	6.73	605	31	57	18.2
451	26	178	0.0422	1.74	2020	526	-1430	-71	5.13	460	55	66	18.1
451	25	184	0.0372	4.97	1230	583	-3500	-86	5.80	504	55	79	18.7
451	25	176	0.0456	7.94	722	569	-5280	-44	5.78	539	55	30	17.5
463	50	26.2	0.0362	1.43	16000	859	-1410	-85	4.01	737	36	122	8.63
463	49	26.1	0.0356	5.06	6610	1230	-3640	-100	4.74	1133	36	94	6.64
463	49	26.1	0.0355	11.6	5030	1370	-8040	-110	5.65	1280	36	90	7.00
463	49	26.2	0.0359	22.4	3450	1360	-14500	-130	5.75	1256	36	106	7.27

Units: T (K); P (Torr); concentrations (10^{13} molecules cm^{-3}); k_{-2}, k_9, k_{10} (s^{-1}); k_2 (10^{-11} cm^3 $molecule^{-1}$ s^{-1}); K_P ($10^5 atm^{-1}$)

Table 5. (continued)

T	P	$[Cl_2CO]$	[Cl]	[MVK]	S_0	Q	λ_1	λ_2	k_2	k_{-2}	k_9	k_{10}	K_P
463	26	97.3	0.0407	0.889	2700	716	-1160	-82	5.23	610	51	107	13.6
463	25	100	0.0442	2.55	2240	747	-2020	-92	5.01	655	51	93	12.1
463	26	97.0	0.0429	4.97	2330	812	-3240	-92	4.81	730	51	82	10.4
463	25	95.1	0.0420	12.9	2690	742	-7700	-49	5.23	713	51	29	11.6
464	101	87.5	0.0357	2.21	2140	1700	-3160	-75	6.70	1603	18	100	6.62
464	101	91.5	0.0396	3.89	1680	2050	-4920	-91	7.41	1948	18	99	6.02
464	100	26.6	0.0391	2.39	3660	2380	-3630	-110	5.44	2184	23	197	3.94
464	100	26.7	0.0387	5.76	4040	2280	-5620	-121	5.81	2156	23	126	4.26
464	100	26.6	0.0388	19.7	3940	2520	-15600	-156	6.52	2397	23	124	4.31
464	12	25.1	0.0343	1.76	12700	401	-920	-84	2.58	361	119	40	11.3
464	12	26.7	0.0353	3.66	12100	524	-1720	-99	3.04	454	119	70	10.6
464	12	26.7	0.0348	6.96	7500	626	-2690	-110	2.79	547	119	79	8.08
464	13	26.5	0.0354	14.6	5470	738	-6000	-121	3.44	645	119	93	8.44
464	12	25.0	0.0341	23.0	4870	699	-9450	-132	3.65	591	119	108	9.76
466	200	23.9	0.0367	2.61	6550	3140	-4720	-94	6.19	2978	15	164	3.27
466	201	24.9	0.0383	5.22	3490	2730	-7490	-127	7.27	3572	15	154	3.20
466	200	23.9	0.0372	9.15	3170	3390	-10300	-142	7.53	3256	15	133	3.64
466	200	23.9	0.0359	13.4	3960	3320	-14400	-143	8.22	3200	15	119	4.04
474	25	70.0	0.0252	1.81	2470	1180	-1910	-94	4.11	1062	49	114	6.00
474	26	69.6	0.0275	2.78	2300	1350	-2640	-104	4.68	1239	49	112	5.85
474	25	66.0	0.0283	5.27	2420	1440	-3730	-114	4.29	1342	49	99	4.96
474	26	62.8	0.0269	9.97	2090	1370	-6220	-110	4.76	1286	49	81	5.74

Units: T (K); P (Torr); concentrations (10^{13} molecules cm^{-3}); k_{-2}, k_9, k_{10} (s^{-1}); k_2 (10^{-11} cm^3 $molecule^{-1}$ s^{-1}); K_P ($10^5 atm^{-1}$)

Table 5. (continued)

T	P	$[Cl_2CO]$	[Cl]	[MVK]	S_0	Q	λ_1	λ_2	k_2	k_{-2}	k_9	k_{10}	K_P
484	26	113	0.0332	1.90	1900	1720	-2390	-113	3.70	1542	52	175	3.64
484	25	115	0.0388	5.45	1990	1920	-4310	-143	4.36	1782	52	138	3.72
484	26	116	0.0300	7.03	1900	2100	-5180	-156	4.36	1953	52	141	3.39
484	26	121	0.0354	9.88	1820	2190	-6540	-168	4.33	2055	52	138	3.20
494	101	258	0.0345	5.22	1720	9650	-12500	-180	5.63	9287	23	360	0.901
494	101	261	0.0349	8.64	1800	9870	-14500	-223	5.45	9582	23	289	0.845
494	101	274	0.0367	14.7	1160	11300	-20200	-342	6.05	10891	23	383	0.826
496	25	292	0.0478	3.73	3460	3300	-4470	-193	3.26	2998	78	298	1.61
496	25	307	0.0412	7.81	3270	3820	-6460	-247	3.44	3554	78	269	1.43
496	25	298	0.0421	15.2	2730	4160	-10100	-320	3.91	3879	78	284	1.49
496	26	302	0.0472	21.9	2410	3970	-12400	-356	3.77	3676	78	290	1.52
509	26	173	0.0375	5.02	3960	5530	-7210	-227	3.43	5169	76	363	0.956
509	26	172	0.0398	10.2	3870	6040	-9420	-315	3.35	5685	76	352	0.850
509	26	168	0.0356	11.2	2500	5800	-9320	-322	3.16	5462	76	334	0.833
509	26	181	0.0213	11.4	3630	6650	-10300	-338	3.21	6279	76	372	0.736

Units: T (K); P (Torr); concentrations (10^{13} molecules cm^{-3}); k_{-2}, k_9, k_{10} (s^{-1}); k_2 (10^{-11} cm^3 $molecule^{-1}$ s^{-1}); K_P ($10^5 atm^{-1}$)

Table 6. Results of Cl + $CH_3C(O)CH=CH_2$ + N_2 ↔ $CH_3C(O)CHCH_2$-Cl + N_2 reaction at 210 K < T < 365 K

T	P	No. Expts.	$[Cl_2CO]$	[Cl]	$[MVK]_{max}$	k_2
214	10	5	36.3	0.017	13	1.91 ± 0.12
215	10	5	60.7	0.037	4	1.71 ± 0.06
215	100	5	73.8	0.049	10	1.71 ± 0.2
217	10	4	137	0.085	13	1.57 ± 0.06
217	50	5	119	0.075	10	1.54 ± 0.03
219	400	5	65.3	0.047	7	1.91 ± 0.06
262	25	5	70.3	0.049	8	1.44 ± 0.04
263	10	5	47.6	0.030	3	1.34 ± 0.02
263	100	4	61.2	0.033	7	1.62 ± 0.04
267	300	4	59.7	0.075	7	1.72 ± 0.13
298 ± 1	10	4	37.4	0.019	2	1.15 ± 0.04
298 ± 1	10	4	26	0.016	10	1.18 ± 0.03
298 ± 1	10	7	40.2	0.017	9	1.25 ± 0.04
298 ± 1	10	4	48.4	0.017	10	1.20 ± 0.09
298 ± 1	10	5	39	0.027	3	1.20 ± 0.03
298 ± 1	25	5	60.1	0.031	6	1.36 ± 0.05
298 ± 1	50	4	6.95	0.021	5	1.60 ± 0.06
298 ± 1	75	5	52	0.033	6	1.49 ± 0.04
298 ± 1	200	5	50	0.030	7	1.62 ± 0.04
298 ± 1	298	5	7.31	0.021	5	1.70 ± 0.08
298 ± 1	601	5	50.9	0.036	6	1.72 ± 0.07
349	300	5	46.2	0.023	10	1.47 ± 0.05
360	300	5	42.8	0.022	9	1.41 ± 0.01
360	600	4	41.2	0.023	11	1.55 ± 0.09
361	10	5	82.7	0.019	6	0.822 ± 0.027
361	25	5	50.7	0.017	9	1.03 ± 0.05
361	51	5	8.04	0.022	5	1.16 ± 0.03
361	100	5	100	0.018	10	1.24 ± 0.06

Units: T (K); P (Torr); concentrations (10^{13} molecules cm^{-3}); k_2 (10^{-10} cm^3 $molecule^{-1}$ s^{-1})

maintained between Cl and $CH_3C(O)CHCH_2$-Cl throughout the course of the reaction at 600 K < T < 760 K and P = 25 – 200 Torr, it can be shown that the correct pseudo-first order rate of reaction of Cl with MVK, k'^{corr}, is related to the observed pseudo-first order rate of reaction, k', as follows:

$$k'^{corr} = (1 + \varepsilon)k' \qquad \text{(XXI)}$$

In the above equation, ε is the equilibrium adduct to Cl concentration ratio as shown in the equation:

$$\varepsilon = [CH_3C(O)CH=CH_2 - Cl]_{eq}/[Cl]_{eq} = K_C[CH_3C(O)CH=CH_2] = K_P[CH_3C(O)CH=CH_2]/RT \qquad \text{(XXII)}$$

For each experimental run at T > 600 K, ε was evaluated using the measured MVK concentration in association with the K_P value obtained by extrapolation of the van't Hoff expression to the appropriate temperature, and a plot of k'^{corr} vs [MVK] was constructed. The magnitude of the slope of the k'^{corr} vs [MVK] plot gives a corrected bimolecular rate coefficient. The magnitude of the correction drops significantly with temperature; it is ~10% at 602K, ~1% at 649 K, and negligible at T > 649 K.

Comparison of rate coefficient for the hydrogen abstraction reaction is labeled k_3^{corr} and k_3^{uncorr} in Table 4. The corrected kinetic data are plotted in Arrhenius form in Figure 7. Therefore, the corrected Arrhenius expression over the temperature range 600 K < T < 760 K is:

$$k_3^{corr}(T) = (5.10 \pm 1.15) \times 10^{-11} \exp[-(1615 \pm 96)/T] \text{ cm}^3 \text{ molecule}^{-1} \text{ s}^{-1} \quad \text{(XXIII)}$$

Errors in the above expression are 2σ and represent precision only.

4.5 $CH_3C(O)CHCH_2$-Cl Thermochemistry: Second-Law Analysis

The equilibrium constants given in Table 5 can be used to obtain information about the thermochemistry of the Cl + $CH_3C(O)CH=CH_2$ ↔ $CH_3C(O)CHCH_2$-Cl using by Equation (X). A van't Hoff plot of ln(K_P) vs versus T^{-1} is shown in Figure 8. The enthalpy change associated with reaction (2) is obtained from the slope of the van't Hoff plot while the entropy change is obtained from the intercept. At 465 K, this 'second-law analysis' gives the results $\Delta_r H = -25.6 \pm 0.9$ kcal mol^{-1} and $\Delta_r S = -28.2 \pm 2.0$ kcal mol^{-1} K^{-1} where the errors are 2σ and represent precision only.

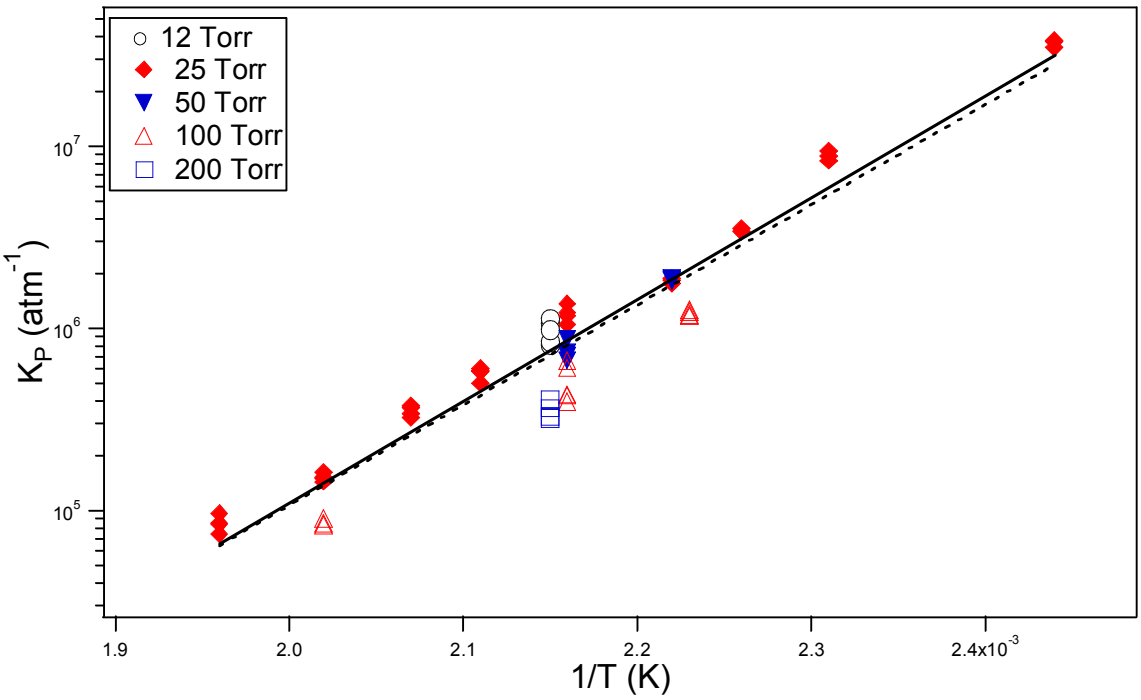

Figure 8. Van't Hoff Plot for the Cl + $CH_3C(O)CH{=}CH_2$ ↔ $CH_3C(O)CHCH_2$-Cl equilibrium

The solid line is obtained from a least squares analysis of K_P versus T^{-1} and gives the second-law thermochemical parameters for the reaction. The dashed line shows the third-law thermochemical parameters for the reaction. Different symbol shapes indicate data obtained at different pressures.

4.6 $CH_3C(O)CHCH_2$-Cl Thermochemistry: Third-Law Analysis

In addition to the second-law analysis, a third law analysis was carried out, where the value of K_P at 465 K (7.24 ± 1.8) x 10^5 atm^{-1} was employed in conjunction with a calculated entropy change to determine $\Delta_r H$ at 465 K for reaction (-2) using equation (X).

Two types of $CH_3C(O)CHCH_2$-Cl adducts are believed possible. Theoretical calculations predict the Cl atom adds either to the terminal or internal carbon on the double bond to form a 2-center – 2-electron bond. However, a significant barrier exists towards occurrence of internal addition as shown in *ab initio* calculations by M.L. McKee of Auburn University that are summarized in Figure 9. Furthermore, as discussed in Section 4.7, product studies suggest that the yield of the terminal addition product is at least 0.75 *[Orlando et al., 2003]*. As for the Cl + MVK reaction, the calculations suggest that the adduct formed by Cl addition to the internal carbon is more stable but will not form efficiently under our experimental conditions.

As mentioned in section 4.2, K_P shows a slight pressure dependence (Figure 8), however, K_P should not depend on inert gas pressure. A possible explanation for this behavior is that there is a significant branching ratio for internal addition, as opposed to the more likely

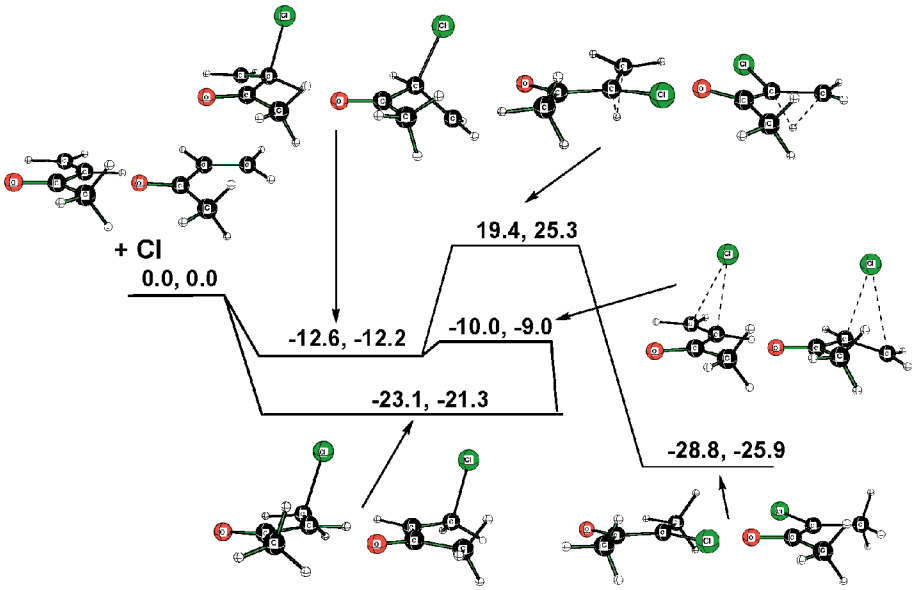

Figure 9. Structure for the Cl + MVK adduct provided by Mike McKee of Auburn University from *ab initio* calculations showing Cl addition to the terminal and internal carbon on the double bond *[McKee, 2008]*

terminal addition, and that the two addition/dissociation reactions have different pressure dependences.

To determine $\Delta_r S$ for reaction (-2), absolute entropies as a function of temperature were obtained from the JANAF tables *[Chase et al., 1985]* for Cl and calculated using *ab initio* vibrational frequencies and moments of inertia for $CH_3C(O)CHCH_2$ and the $CH_3C(O)CHCH_2$-Cl adduct provided McKee. We assume formation of the terminal addition product in this analysis. Important parameters used in calculations of absolute entropies and heat capacity corrections are summarized in Table 7. At 465 K, the third law analysis gives $\Delta_r H = -24.5 \pm 1.8$ kcal mol^{-1} and $\Delta_r S = 25.5 \pm 2.4$ cal mol^{-1} K^{-1}; the uncertainties reported represent an estimate of the imperfect knowledge of the input data needed to calculate absolute entropies (particularly the low-frequency $CH_3C(O)CHCH_2$-Cl vibrations) as well as the uncertainty in the experimental value for K_P at 465 K.

Heat capacity corrections have been employed to determine $\Delta_r H°$ values at 298 K and 0 K; results are given in Table 8. The thermochemical parameters determined by the second and third-law analyses are in very good agreement as compared in Table 8. Uncertainties listed in Table 3 are accuracy estimates at the 95% confidence level. The values for $\Delta_r H°$ can be used in conjunction with literature values for standard enthalpies of formation of Cl *[Chase et al., 1985]* and MVK *[Guthrie, 1978]* to deduce

Table 7. Summary of parameters used in calculations of absolute entropies and heat capacity corrections for the Cl +$CH_3C(O)CH=CH_2$ ↔ $CH_3C(O)CHCH_2$-Cl reaction

	Cl	**$CH_3C(O)CH=CH_2$**	**$CH_3C(O)CHCH_2$-Cl**
g_0	4	1	2
g_1	2		
$\Delta\varepsilon/cm^{-1a}$	882.36		
σ		2	2
Rot. Constants/cm^{-1b}		0.296, 0.147, 0.0973	0.228, 0.0427, 0.0400
Vib. Frequencies/cm^{-1b}		110, 124, 276, 431, 491, 536, 697, 766, 955, 987, 1037, 1057, 1080, 1282, 1317, 1411, 1459, 1495, 1501, 1690, 1753, 3052, 3110, 3163, 3167, 3187, 3247	40, 51, 90, 243, 293, 422, 515, 582, 637, 714, 807, 966, 993, 1038, 1119, 1184, 1224, 1290, 1409, 1434, 1489, 1496, 1499, 1622, 3047, 3105, 3107, 3160, 3187, 3199

[a] $\Delta\varepsilon$ ≡ energy splitting between the lowest two electronic states; both $CH_3C(O)CH=CH_2$ and $CH_3C(O)CHCH_2$-Cl are assumed to have no energetically accessible excited electronic states.

[b] Calculated values at the B3LYP/6-31+G(d)+ZPC level of theory.

Table 8. Thermochemical parameters for the reaction Cl + $CH_3C(O)CH=CH_2 \leftrightarrow CH_3C(O)CHCH_2$-Cl

T	Method	$-\Delta_rH$	$-\Delta_rS$
465	2nd law	25.6 ± 0.9	28.2 ± 2.0
	3rd law	24.5 ± 1.8	25.5 ± 2.4
298	2nd law	25.5 ± 0.9	27.9 ± 2.0
	3rd law	24.5 ± 1.8	25.2 ± 2.4
0	2nd law	25.0 ± 0.9	
	3rd law	24.0 ± 1.7	
	B3LYP/6-31+G(d)+ZPC (anti conformer)	23.1	
$\Delta H_{f,298}$ ($CH_3C(O)CHCH_2$-Cl) = 31.5 ± 3.3			

Units: T (K); P (Torr); ΔH, $\Delta H_{f,T}$ (kcal mol^{-1}); ΔS (cal mol^{-1} K^{-1})

the values for the standard enthalpy of formation of $CH_3C(O)CHCH_2$-Cl, also given in Table 8.

4.7 Literature Comparison

In 1999, Canosa-Mas et al. *[1999]* studied the gas-phase reaction of Cl radicals with methylvinyl ketone using a relative rate technique at atmospheric pressure and ambient temperature. Four different reaction mixtures were used in this study. Three experiments used N_2 as the bath gas while the other used synthetic air. The photolyte used in this study was molecular chlorine. Products in the reaction mixture were followed by gas

chromatography coupled with flame-ionization detection. The rate coefficient obtained for the reaction was (2.0 ± 0.5) x 10^{-10} cm^3 $molecule^{-1}$ s^{-1}.

Additionally, in 2001, Canosa-Mas et al. *[2001]* studied the gas-phase reaction of Cl radicals with MVK using the absolute technique of discharge-flow at a pressure of 1.6 Torr of helium and 4.5 Torr of nitrogen at room temperature. The source of Cl atoms was the reaction of HCl with atomic fluorine. Final products formed in the reaction mixture were determined using FT-IR spectroscopy. The rate coefficient obtained for the reaction was (0.99 ± 0.20) at 1.6 Torr and (1.1 ± 0.3) at 4.5 Torr both in units of 10^{-10} cm^3 $molecule^{-1}$ s^{-1}. Comparing the rate coefficients of this study to both Canosa-Mas et al. *[1999]* and *[2001]* shows excellent agreement as can be compared in Table 9 for reactions around room temperature.

Another relative rate study was conducted in 1999 by Finlayson-Pitts et al. *[1999]*, who studied the same reaction at 298 K and 1 atm pressure in N_2. Chlorine radicals were generated by photolysis of CCl_3COCl to give a rate coefficient of (2.0 ± 0.2) x 10^{-10} cm^3 $molecule^{-1}$ s^{-1}. In contrast to Canosa-Mas et al. *[1999]*, Finlayson-Pitts et al. *[1999]* states that Cl_2 could not be used as a chlorine atom source because it reacts in the dark with the MVK. Product species were followed using gas chromatography with

flame ionization detection. Again, excellent agreement is maintained with the rate coefficients determined in this study.

In 2003, Orlando et al. *[2003]* studied the gas-phase reaction of Cl radicals with methylvinyl ketone in which rate coefficients were determined using FT-IR spectroscopy and the relative rate technique at 298 K and 700 Torr of synthetic air. The photolyte used in this study was molecular chlorine. The rate coefficient obtained for the reaction was $(2.2 \pm 0.3) \times 10^{-10}$ cm^3 $molecule^{-1}$ s^{-1}.

In addition to determining the rate coefficient, Orlando et al. *[2003]* carried out product yield experiments at 298 K and 720 Torr in synthetic air in which several key species were observed; chloroacetaldehyde, CO_2, CH_2O, CH_3OH, HCOCl, and peracetic acid were quantified by either spectral stripping routines or infrared absorption cross-section data. The large yield of chloroacetaldehyde, as indicated by the authors, suggests the majority of chlorine (at least 75%) adds to the terminal carbon on the site of unsaturation as seen in reaction (2). Conversely, reaction by internal addition, as shown below, is believed to be minor product due to the very low observed HCOCl yield.

$$Cl + CH_3C(O)CH=CH_2 + N_2 \leftrightarrow CH_3C(O)C(Cl)HCH_2 + N_2 \qquad \text{(XXIV)}$$

A comparison of rate coefficients from this study to Orlando et al. *[2003]* shows excellent agreement. Similarly to Orlando et al. *[2003]*'s product study, *ab initio* structural and energetic calculations for the Cl + MVK reaction at B3LYP/6-31+G(d)+ZPC level of theory carried out by McKee, as seen in Figure 9, also show internal addition as a possible product: however, a significant barrier exists toward its formation.

For further comparison, Table 9 gives the rate coefficients obtained from this study over the temperature range 210 K < T < 365 K and pressure range 10 Torr ≤ P ≤ 600 Torr as compared to the four studies mentioned above. Again, excellent agreement between these studies is observed for experiments performed around room temperature.

Bond strengths for other adducts formed in reactions of Cl with olefins have been reported and can be compared to reaction with MVK. *Ab initio* calculations were carried out by Schlegel et al., *[1984]* to determine the bond strength of the ethene-Cl adduct. The authors optimized geometries and transitional structures with 3-21G and 6-31G basis sets. Energies were computed using Hartree-Fock and Moller-Plesset methods which calculated $\Delta_r H = -17$ kcal mol^{-1} at 298 K. Nicovich et al. *[1996]* employed the LFP-RF technique to study the reaction of Cl + tetrachloroethylene (C_2Cl_4) as a function of temperature (231 – 290 K) and pressure (3 – 700 Torr) in N_2 bath gas. These authors obtained $\Delta_r H = -(18.1$

± 1.3) kcal mol^{-1} for this reaction at 298 K. The importance of bond strength comparisons for Cl + MVK to other unsaturated species are addressed in Chapter 5.

Table 9. Comparison of results for the Cl + $CH_3C(O)CH=CH_2 \leftrightarrow$ $CH_3C(O)CHCH_2$-Cl reaction from this study to existing literature studies

Source	T	P	Expt. Technique	Bath Gas	k2
This study	214	10	LFP-RF	N_2	1.91 ± 0.12
This study	215	10	LFP-RF	N_2	1.71 ± 0.06
This study	215	100	LFP-RF	N_2	1.71 ± 0.2
This study	217	10	LFP-RF	N_2	1.57 ± 0.06
This study	217	50	LFP-RF	N_2	1.54 ± 0.03
This study	219	400	LFP-RF	N_2	1.91 ± 0.06
This study	262	25	LFP-RF	N_2	1.44 ± 0.04
This study	263	10	LFP-RF	N_2	1.34 ± 0.02
This study	263	100	LFP-RF	N_2	1.62 ± 0.04
This study	267	300	LFP-RF	N_2	1.72 ± 0.13
Canosa-Mas et al., 2001	298 ± 1	1.6	discharge-flow	He	0.99 ± 0.2
Canosa-Mas et al., 2001	298 ± 1	4.5	discharge-flow	N_2	1.1 ± 0.3
This study	298 ± 1	10	LFP-RF	N_2	1.15 ± 0.04
This study	298 ± 1	10	LFP-RF	N_2	1.18 ± 0.03
This study	298 ± 1	10	LFP-RF	N_2	1.25 ± 0.04
This study	298 ± 1	10	LFP-RF	N_2	1.20 ± 0.09
This study	298 ± 1	10	LFP-RF	N_2	1.20 ± 0.03

Units: T (K); P (Torr); k_2 (10^{-10} cm^3 $molecule^{-1}$ s^{-1})

Table 9. (continued)

Source	T	P	Expt. Technique	Bath Gas	k2
This study	298 ± 1	25	LFP-RF	N_2	1.36 ± 0.05
This study	298 ± 1	50	LFP-RF	N_2	1.60 ± 0.06
This study	298 ± 1	75	LFP-RF	N_2	1.49 ± 0.04
This study	298 ± 1	200	LFP-RF	N_2	1.62 ± 0.04
This study	298 ± 1	298	LFP-RF	N_2	1.70 ± 0.08
This study	298 ± 1	601	LFP-RF	N_2	1.72 ± 0.07
Orlando et al., 2003	298	700	relative rate	synth. air	2.2 ± 0.3
Canosa-Mas et al., 1999	298 ± 1	760	relative rate	N_2	2.0 ± 0.5
Finlayson-Pitts et al., 1999	298	760	relative rate	N_2	2.0 ± 0.2
This study	349	300	LFP-RF	N_2	1.47 ± 0.05
This study	360	300	LFP-RF	N_2	1.41 ± 0.01
This study	360	600	LFP-RF	N_2	1.55 ± 0.09
This study	361	10	LFP-RF	N_2	0.822 ± 0.027
This study	361	25	LFP-RF	N_2	1.03 ± 0.05
This study	361	51	LFP-RF	N_2	1.16 ± 0.03
This study	361	100	LFP-RF	N_2	1.24 ± 0.06

Units: T (K); P (Torr); k_2 (10^{-10} cm^3 $molecule^{-1}$ s^{-1})

CHAPTER 5

CONCLUSIONS

The laser flash photolysis – resonance fluorescence (LFP-RF) technique was employed to study the following reactions over a range of temperatures and pressures:

$$Br + CH_3C(O)CH=CH_2 + N_2 \leftrightarrow CH_3C(O)CHCH_2\text{-}Br + N_2 \quad (1, -1)$$

$$Cl + CH_3C(O)CH=CH_2 + N_2 \leftrightarrow CH_3C(O)CHCH_2\text{-}Cl + N_2 \quad (2, -2)$$

$$Cl + CH_3C(O)CH=CH_2 \rightarrow \dot{C}H_2C(O)CH=CH_2 + HCl \quad (3)$$

Reactions (1) and (2) display similar kinetics, but over different temperature regimes. Reversible addition of Br to MVK was observed over the 200 K < T < 250 K range for the experimental conditions employed. At temperatures above 298 K no reaction of Br with MVK was observed. In the case of the Cl + MVK reaction, reversible addition was observed over the 405 K < T < 510 K range and stable addition at lower temperatures 210 K < T < 365 K. Measurement of k_i/k_{-i} (i = 1, 2) as a function of temperature provides temperature-dependent equilibrium data from which thermochemical parameters can be obtained. Second and third-law

analyses of the equilibrium data yields the following results: for Br addition to MVK, $\Delta_rH°_{298} = -11.4 \pm 0.8$ kcal mol^{-1}, $\Delta_rH°_0 = -11.0 \pm 0.7$ kcal mol^{-1}, $\Delta_rS°_{298} = -25.0 \pm 2.6$ cal mol^{-1} K^{-1}, whereas for Cl, $\Delta_rH°_{298} = -25.0 \pm 2.0$ kcal mol^{-1}, $\Delta_rH°_0 = -24.5 \pm 1.9$ kcal mol^{-1}, $\Delta_rS°_{298} = -26.6 \pm 3.1$cal mol^{-1} K^{-1}.

The kinetics of reactions (1, -1) represents the first direct study of these reactions. Sauer et al. *[1999]* conducted the only other gas kinetics study of the Br + MVK reaction. However, their experiments were carried out using the indirect relative rate technique at 301 ± 3 K in 1 atm synthetic air. Due to the reaction of O_2 with the MVK-Br adduct, reaction (I), this study could not be directly compared to Sauer et al. *[1999]*. However, as explained in section 3.4, the rate coefficient for reaction (I) was estimated using the results from our study in conjunction with those from the Sauer et al. *[1999]* study, and was found to be ~1.4 x 10^{-13} cm^3 molecule^{-1} s^{-1} at T = 301 ± 3 K and P = 1 atm synthetic air. Rate coefficients for the reaction of other olefin-Br adducts with oxygen was conducted by Catoire et al., *[1997] and* Ramacher et al., *[2000];* similar values for the rate coefficient as compared to our estimate was obtained. Therefore, our estimate for the rate at which the MVK-Br adduct reacts with oxygen is reasonable.

Comparison with the product study for reaction (1) conducted by Sauer et al. *[1999]* with *ab initio* structural and energetic calculations for

the Br and MVK reaction shown in Figure 4 show good agreement in that both indicate that terminal addition should dominate.

The reaction of Cl with MVK, has been studied over the temperature and pressure ranges 210 K < T < 760 K and 10 ≤ P ≤ 600 Torr. This represents the first comprehensive examination of the Cl + MVK reaction. Four existing gas kinetic studies have been conducted previously. Canosa-Mas et al. *[1999]*, Finlayson-Pitts et al. *[1999]*, and Orlando et al. *[2003]* have only studied the reaction at room temperature and ~1 atm using relative rate techniques, while Canosa-Mas et al. *[2001]* investigated the reaction at room temperature in 1.6 Torr He and 4.5 Torr N_2 using an absolute technique. Excellent agreement is observed among the four room temperature studies and this study.

Comparing Orlando et al. *[2003]*'s product study to *ab initio* structural and energetic calculations for the Cl and MVK reaction at B3LYP/6-31+G(d)+ZPC level of theory carried out by McKee *[2008]* also shows the potential for formation of both internal and terminal addition products. However, a significant barrier exists toward internal addition as shown in Figure 9. Additionally, a slight pressure dependence of K_P was observed by the Cl and MVK reaction shown in Figure 8. A possible explanation could be that the internal and terminal addition/dissociation reactions have different pressure dependences. We conclude that while

terminal addition appears to be most important, internal addition could be a significant minor pathway.

A hydrogen abstraction reaction was only observed at high temperatures, 600 K < T < 760 K, and only for Cl + MVK. The resulting Arrhenius expression, corrected for the addition reaction (2), adequately describes all kinetic data over the temperature range 600 K < T < 760 K for reaction (3) as shown below:

$$k_3^{corr}(T) = (5.10 \pm 1.15) \times 10^{-11} \exp[-(1615 \pm 96)/T] \text{ cm}^3 \text{ molecule}^{-1} \text{ s}^{-1} \quad \text{(XXIII)}$$

Orlando et al. *[2003]* did not discuss any evidence toward the formation of hydrogen abstraction reaction at 298 K and 720 Torr (synthetic air) in their product study. At present, no other scientific study exists for reaction (3) or any possible hydrogen abstraction with Br and MVK, which is sufficiently endothermic that it could only occur at a measurable rate at very high temperatures. However, the high temperature results for the Cl + MVK reaction from this study can be extrapolated to room temperature using equation (XXIII) to yield a rate coefficient of 2.3×10^{-13} cm^3 molecule^{-1} s^{-1}. Therefore, this study suggests that the H-abstraction branching ratio at T = 298 K and P = 1 atm is around 0.1%.

Comparisons of bond strengths for the MVK-Br adduct to other olefin-Br adducts shows the MVK-Br adduct to be the most strongly bound of the ones studied to date. This property has important ramifications for Br chemistry in the atmosphere. As discussed in section 3.4, a fraction (~1/3) of MVK-Br adduct molecules react with O_2 at 301 K and 1 atm air to form a peroxy radical with the other 2/3 being lost via unimolecular decomposition. The fraction that reacts with O_2 will become larger at lower temperatures observed in the troposphere. The bond strength of the Br adduct is the most important factor influencing the competition between adduct dissociation and adduct reaction with O_2, and it is this competition along with the association rate coefficient (k_1) that controls the rate of Br-initiated destruction of MVK in the atmosphere. In contrast to Br adduct reactions with O_2, the Cl adducts discussed in section 4.7 are much stronger and essentially all react completely with O_2. The limited available data concerning bond strengths for Br + olefin and Cl + olefin adducts are consistent with the expectation that substitution of electron-donating groups on the double bond carbons increases adduct stability whereas substitution of electron-withdrawing groups reduces adduct stability.

Future research should include a more thorough examination of the pressure dependence observed for K_P in the Cl + MVK equilibrium reaction

as shown in Figure 8. As stated earlier, K_P should not depend on inert gas pressure. Expanding the range of pressures studied over the observed equilibrium temperature regime could help provide helpful evidence to support that the site of addition to the double bond in MVK may be pressure dependent. Additional direct measurements of bond dissociation energies, particularly for Br + Olefin adducts, would also be of importance in improving our understanding of this important class of atmospheric reactions.

REFERENCES

Atkinson, R., *Chem. Rev*. **1986**, *86*, 69.

Barnes, I., Bastian, V., Becker, K.H., Overath, R., and T. Zhu, *Int. J. Chem. Kinet***. 1989,** *16*, 545.

Barrie, L.A., Bottenheim, J.W., Schnell, R.C., Crutzen, P.J., and R.A. Rasmussen, *Nature*. **1988**, *334*, 138.

Bedjanian, Y., Poulet, G., and G. Le Bras, *J. Phys, Chem. A*. **1998**, *102*, 5867.

Bedjanian, Y., Poulet, G., and G. Le Bras, *J. Phys, Chem. A*. **1999**, *103*, 4026.

Bedjanian, Y., Poulet, G., and G. Le Bras, *J. Phys, Chem. A*. **2000**, *104*, 577.

Boundries, H., and J.W. Bottenheim, *Geophys. Res. Lett*. **2000**, *27*, 517.

Braun, W., and M. Lenzi, Discuss. *Faraday Soc*. **1967**, *44*, 252.

Canosa-Mas, C.E., Cotter, E.S.N., Duffy, J., Thompson, K.C., and R.P. Wayne, *Phys. Chem. Chem. Phys*. **2001**, *3*, 3075.

Canosa-Mas, C.E., Hutton-Square, H.R., King, M.D., Stewart, D.J., Thompson, K.C., and R.P. Wayne, *J. Atmos. Chem.* **1999**, *34*, 163.

Catoire, V., Ariya, P.A., Niki, H., and G.W. Harris, *Int. J. Chem. Kinet***. 1997,** *29*, 695.

Chase, Jr, M.W., Davies, C.A., Downey, Jr, J.R., Frurip, D.J., McDonald, R.A., and A.N. Syverud, *J. Phys. Chem. Ref. Data*. **1985**, *14*(Suppl. 1).

Chichinin, A.I., *Chem. Phys. Lett*. **1993**, *209*, 459.

Chichinin, A.I., *J. Phys. Chem. Ref. Data*. **2006**, *35*, 869.

Ferrell, V., Master's Thesis, *Georgia Institute of Technology*. **1998**.

Finlayson-Pitts, B.J., and J.N. Pitts Jr., *Chemistry of the Upper and Lower Atmosphere*, *Academic Press: San Diego*. **2000**, 146.

Finlayson-Pitts, B.J., Keoshian, C.J., Buehler, B., and A. Ezell, *Int. J. Chem. Kinet*. **1999,** *31*, 491.

Finlayson-Pitts, B.J., *Res. Chem. Intermed.* **1993**, *19*, 235.

Gierczak, T., Burkholder, J.B., Talukdar, R.K., Mellouki, A., Barone, S.B., and A.R. Ravishankara, *J. Photochem. Photobiol. A: Chem*. **1997**, *110*, 1.

Guthrie, J.P., *Can. J. Chem*. **1978**, *56*, 962.

Hsin, H.Y, and M.J. Elrod, *J. Phys, Chem. A*. **2007**, *111*, 613.

Isidorov, V.A., Zenkevich, I.G., and B.V. Ioffe, *Atmos. Environ*. **1985**, *19*, 1.

Jobson, B.T., Niki, H., Yokouchi, Y., Bottenheim, J., Hopper, F., and R. Leaitch, *J., Geophys. Res.* **1994**, *99*, 25355.

Johnson, R.O., Perram, G.P., and W.B. Roh, *J. Chem Phys.* **1996**, *104*, 7052.

Maul, C., Haas, T., Gericke, K.H., and F.J. Comes, *J. Chem. Phys.* **1995**, *102*, 3238.

McKee, M., Personal coorespondance with Dr. Paul Wine. **2008**.

Nicovich, J.M., Wang, S., McKee, M.L., and P.H. Wine, *J. Phys, Chem.* **1996**, *100*, 680.

Ochando-Pardo, M., Nebot-Gil, I., González-Lafont, Á., and J.M. Lluch, *Chem. Phys. Lett*. **2005**, *409*, 255.

Orlando, J.J., Tyndall, G.S., Apel, E.C., Riemer, D.D., and S.E. Paulson, *Int. J. Chem. Kinet*. **2003,** *35*, 334.

Peterson, A.B., Wittig, C., and S.R. Leone, *Applied Phys. Lett.* **1975**, *27*, 305.

Platt, U., and Janssen, C., Faraday Discuss. **1995**, *100*, 175.

Pszenny, A.A.P., Keene, W.C., Jacob, D.J., Fan, S., Maben, J.R., Zetwo, M.P., Springer-Young, M., and J.N. Galloway, *Geophys. Res. Lett*. **1993**, *20*, 699.

Raber, W.H., and Moortgat G.K., *Progress and Problems in Atmospheric Chemistry, Editor, John R. Barker, World Scientific: Singapore*. **1995**, *Vol. 3*, 318.

Ragains, M.L., and B.J. Finlayson-Pitts, *J. Phys. Chem. A*. **1997**, *101*, 1509.

Ramacher, B., Orlando, J.J., and G. Tyndall, *Int. J. Chem. Kinet***. 2000,** *33*, 198.

Ramacher, B., Rudolph, J., and R.J. Koppmann, *Tellus*. **1997**, 49B, 607.

Rudolph, J., Koppmann, R., and C.H., Plass-Dülmer, *Atmos. Environ*. **1996**, *30*, 1887.

Sauer, C.G., Barnes, I., and K.H. Becker, *Atmos. Environ***. 1999**, *33*, 2969.

Schlegel, H.B., and C. Sosa, *J. Phys. Chem*. **1984**, *88*, 1141.

Singh, H.B., Gregory, G.L., Anderson, B., Browell, E., Sachse, G.W., Davis, D.D., Crawford, J., Bradshaw, J.D., Talbot, R., Blake, D.R., Thornton, D., Newell, R., and J. Merrill, *J. Geophys. Res.* **1996a**, *101*, 1907.

Singh, H.B., Thakur, A.N., Chen, Y.E., and Kanakidou, M., *Geophys. Res. Lett.* **1996b**, *23*, 1529.

Sturges, W.T., and G.E. Shaw, *Atmos. Environ*. **1993a**, *27A*, 2969.

Sturges, W.T, Cota, G.F., and P.T. Buckley, *Nature*. **1992**, *358*, 660.

Sturges, W.T., Schnell, R.C., Dutton, G.S., Garcia, S.R., and J.A. Lind, *Geophys. Res. Lett*. **1993b**, *20*, 201.

Tang, T., and J.C. McConnell, *Geophys. Res. Lett*. **1996**, *23*, 2633.

Tauzon, E.C., and R. Atkinson, *Int. J. Chem. Kinet***. 1989,** *21*, 1141.

Tyndall, G.S., Orlando, J.J., Kegley-Owen, C.S., *J. Chem. Soc. Far. Trans.* **1995**, *91*, 3055.

Vogt, R., Crutzen, P.J, and R. Sander, *Nature*. **1996**, *383*, 327.

Wingenter, O.W., Sive, N.J., Blake, N.J, Blake, D.R., and F.S. Rowland, *J. Geophys. Res. Atmos*. **2005**, *110,* D20308, doi:10.1029/2005JD005875.

Zhao, Z., Huskey, D.T., Olsen, K.J., Nicovich, J.M., McKee, M.L., and P.H. Wine, *Phys. Chem. Chem. Phys*. **2007**, *9*, 4383.